

Post-SELEX modification of aptamers through reversible formation of N-methoxy-1,3-oxazinane (MOANA) nucleoside analogues

Muditha Herath

Master's Thesis

Department of Chemistry

Faculty of Science

University of Turku

July 2024

The originality of this thesis has been checked in accordance with the University of Turku quality assurance system using the Turnitin OriginalityCheck service.

UNIVERSITY OF TURKU

Department of Chemistry

HERATH, MUDITHA: Post-SELEX modification of aptamers through reversible formation of N-methoxy-1,3-oxazinanone (MOANA) nucleoside analogues.

Master's Thesis, 34p, 17 app. p.

July 2024

The effective use of aptamers has been developed significantly in the recent past due to their widespread applications in areas such as therapeutics, biosensors and nanotechnological applications. Due to this increasing demand, researchers are continuously engaged in modifying aptamers to ensure a strong and selective binding with the targets. Apart from the general SELEX method, post-SELEX modifications have become more efficient to develop aptamer libraries which can efficiently bind with the target.

Out of the different types of aptamers which can be further modified, the “cocaine binding aptamer” (MN4) can be identified as a prominent candidate. Even though MN4 was originally developed to bind with cocaine, it has a higher affinity towards the “off-target” quinine. Therefore, quinine was used as the target ligand in this project. Previous studies have reported several investigations on binding of different quinine derivatives to the cocaine aptamer. However, there is no literature on screening for aptamer-aldehyde combinations with improved binding affinity for quinine.

In this work, the effect of modifications at the binding site on the binding affinity of MN4 was examined. By replacing any of the three pre-determined nucleotides of the aptamer by benzylidene protected (2R,3S)-4-(methoxyamino)butane-1,2,3-triol phosphoramidite (a MOANA residue), three different modified aptamers (T19, C20 and A21) were synthesized. Further elaboration was carried out by reacting the aptamers with selected mixtures of aldehydes, in the presence and absence of quinine. The reaction was carried out at pH 5.5 and room temperature to promote reversible formation of respective MOANA analogues. Further analysis by UHPLC/MS showed promising results for the C20 scaffold with methyl-4-formylbenzoate and 3-nitrobenzaldehyde derivatives.

Keywords: aptamers, post-SELEX modifications, 1,3-oxazinanones, derivatization

Table of Contents

1. Introduction.....	1
1.1 Aptamers.....	1
1.2 Cocaine binding aptamers.....	1
1.2.1 Off-target binding of cocaine aptamer.....	2
1.3 Screening of aptamers.....	3
1.3.1. Drawbacks of conventional SELEX.....	4
1.4 post-SELEX modifications.....	5
1.4.1. Chemical modifications.....	6
1.4.2. Truncation and optimization.....	8
1.4.3. Limitations of post-SELEX modifications.....	8
1.5 Dynamic Combinatorial Chemistry.....	9
1.5.1. General principles of DCC.....	9
1.5.2. Coupling reactions.....	10
1.5.3. Applications of DCC.....	11
1.6 1,3-Oxazinanes and the reactions.....	12
1.7 Purpose of the research work.....	14
2. Results and discussion.....	15
2.1 Oligonucleotide synthesis.....	15
2.1.1. Purification of the modified aptamers.....	16
2.2 Selection of aldehydes for the DCC experiments.....	21
2.3 Derivatization of modified aptamers with aldehydes.....	24
2.4. Isothermal Titration Calorimetric studies.....	28
3. Experimental.....	29
3.1 General methods and materials.....	29
3.2 Synthesis of modified aptamers.....	30
3.3 Derivatization of modified aptamers with aldehydes.....	31
3.3.1 Preparation of aldehyde samples.....	31
3.3.2 Incubation with aldehydes at pH 5.5.....	32
3.4 Isothermal Titration Calorimetric studies.....	32
3.4.1 Preparation of samples and purification.....	32
3.4.2 ITC studies.....	33

4. Summary and Conclusion.....	33
5. References.....	35
6. Appendices.....	41

Abbreviations and Acronyms

ACN	Acetonitrile
CE-SELEX	Capillary Electrophoresis SELEX
CPG	Controlled Pore Glass
DMSO	Dimethyl sulphoxide
DMTr	4,4-dimethoxytrityl
DNA	Deoxyribonucleic Acid
ED	Electron Donating
EW	Electron Withdrawing
FDA	Food and Drug Administration
HFIP	Hexafluoro isopropanol
¹ H-NMR	Hydrogen Nuclear Magnetic Resonance
IP-SELEX	Immunoprecipitation coupled SELEX
ITC	Isothermal Titration Calorimetry
LNA	Locked Nucleic Acid
MOANA	<i>N</i> -methoxy-1,3-oxazinane nucleic acid
ON	Oligonucleotide
³¹ P-NMR	Phosphorus Nuclear Magnetic Resonance
PCR	Polymerase Chain Reaction
RNA	Ribonucleic Acid
RP-HPLC	Reverse Phase High Performance Liquid Chromatography
SELEX	Systematic Evolution of Ligands by Exponential enrichment.
TEAA	Triethylammonium acetate
TNA	Threose Nucleic Acid
UHPLC-MS	Ultra High Performance Liquid Chromatography – Mass Spectrometry
VEGF	Vascular Endothelial Growth Factor

1 Introduction

1.1 Aptamers

Aptamers are short sequences of DNA, RNA or synthetic nucleic acids which can bind to specific target molecules. They can bind to a range of targets such as proteins, carbohydrates, peptides, single cells or even tissues. They were first discovered in 1990 and often referred as “chemical antibodies” due to their similarity with antibodies in binding affinity and specificity.^{1,2} However, compared to the antibodies, aptamers show higher stability and lower immunogenicity towards a target ligand.³ Also, the production of aptamers is advantageous as it is more cost-effective and less time consuming. Moreover, aptamers can be modified easily than antibodies, and the variation from batch to batch is significantly lower in aptamers.⁴ Considering all these advantages, aptamers are being used in numerous applications such as therapeutics,⁵⁻⁹ diagnostics,¹⁰⁻¹² biosensors¹³⁻¹⁵ and many other pharmaceutical applications. The demand for the applications of aptamers is increasing significantly over the recent years due to their effectiveness.

The structure of the aptamer plays an important role when binding with the targets. When aptamers bind to the target, their structure changes and folds into a 3D structure as a response to the target. This formation of 3D structure enables the target specificity of the aptamer. Therefore, the whole sequence of the aptamer would not be essential for binding specificity as some regions of the aptamer do not possess binding sites. So, the tertiary structure is more important in binding, than the whole sequence of the aptamer.^{16,17}

1.2 Cocaine binding aptamer

Cocaine binding aptamer is a DNA aptamer consisting of three stems which originate from a three-way junction. Out of the different types of aptamers, the cocaine binding aptamer can be identified as a prominent candidate for numerous applications in biosensing¹⁸ and drug delivery methods.¹⁹ It has been reported that the structure changing mechanisms of cocaine aptamer are responsible for this variety of applications.²⁰ Since the cocaine binding aptamer is a three-way junction aptamer, the three stems are

structured in different spatial formats by offering different structures such as MN19, MN1 and MN4. When the stem to the left is shortened into three base pairs, the MN19 structure is formed. The MN1 and MN4 were almost similar in structures but MN1 has two additional Watson-Crick base pairings than MN4. Out of these structures, the MN4 aptamer shows the least variation when it binds with the target ligand.²¹ Also, a previous study on thermodynamic analysis of cocaine aptamers reported that the MN4 structure has improved binding affinity towards the targets compared to the other structures.²² Figure 1 below shows the 2D structures of MN4, MN1 and MN19 aptamers.

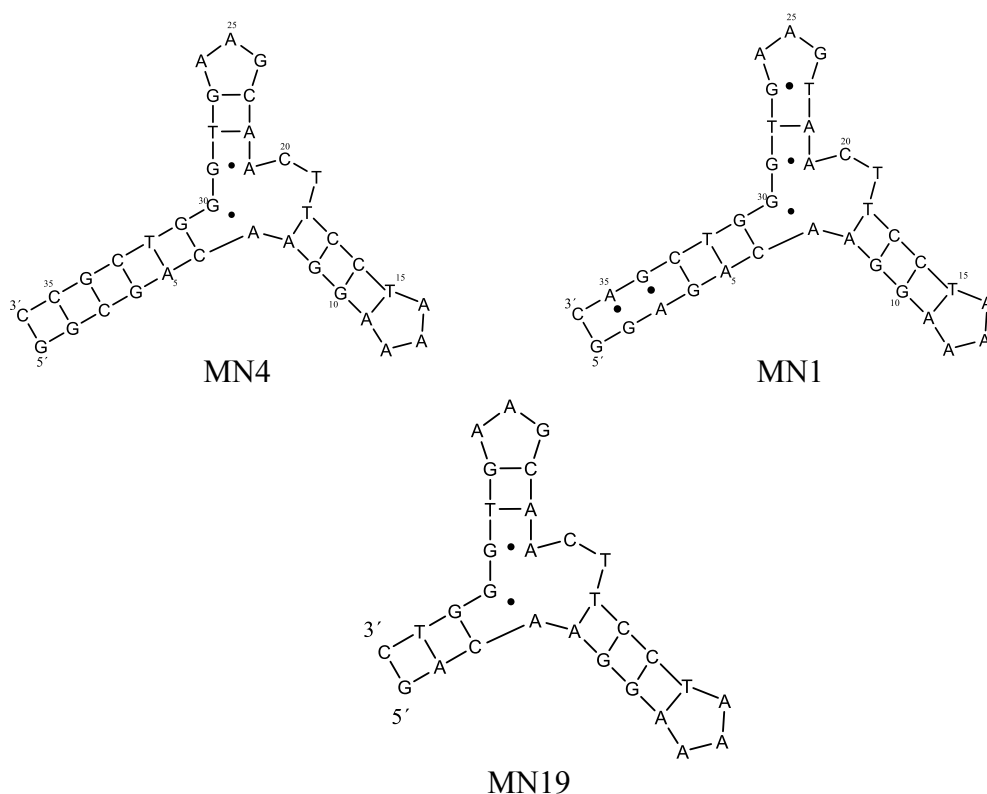


Figure 1. 2D illustrations of MN4, MN1 and MN19 structures of cocaine binding aptamer. The dashes represent Watson-Crick base pairs, while the dots represent non Watson-Crick base pairs.

1.2.1 Off-target binding of Cocaine aptamer

Aptamers are typically identified as specific towards a certain target molecule. However, the cocaine binding aptamer tends to bind with other targets with a higher affinity than the desired target, cocaine. One of the most notable off-targets is quinine. It has been reported that quinine tends to bind with the cocaine aptamer more than 30 times stronger

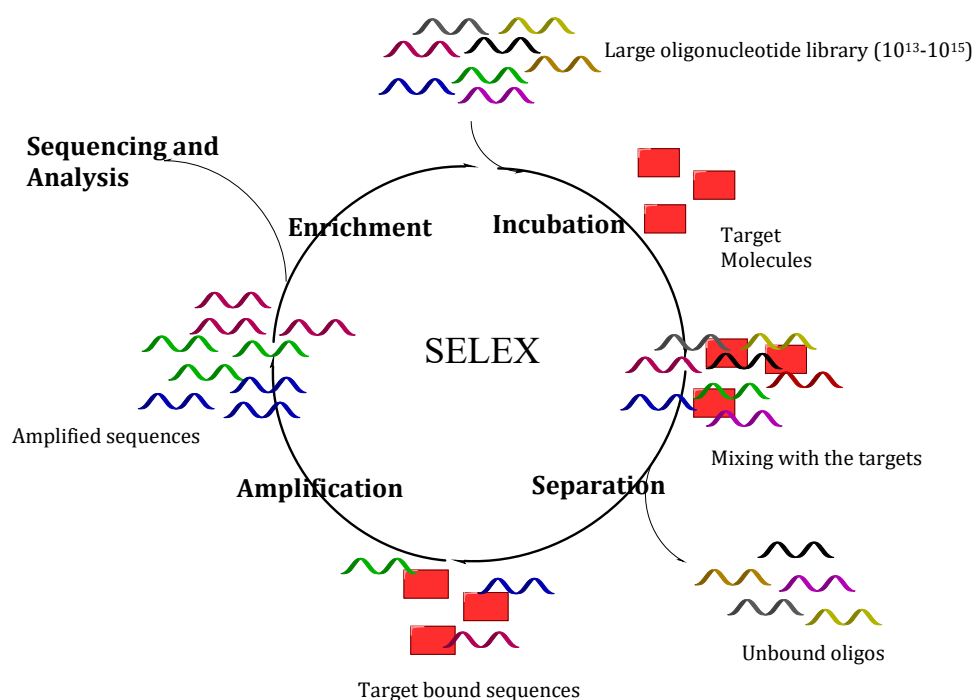
than cocaine.^{23–27} Such affinity towards an off-target is unusual for an aptamer. However, this behaviour can be taken as an advantage to investigate other possible ligands that could bind with this aptamer.



Figure 2. Chemical structure of A) Cocaine, B) Quinine

1.3 Screening for aptamers

The selection of aptamers is performed by a process called “SELEX” (Systematic Evolution of Ligands by Exponential enrichment) which was first reported in the 1990s.²⁸ The process starts by synthesizing a large diverse pool of oligonucleotides, typically 10^{13} – 10^{15} different sequences. Then the library is incubated with the target molecule. Sequences that bind to the target are separated from non-binders. Then the bound sequences are amplified using PCR and the process is repeated for multiple rounds to enrich the pool with high-affinity binders.



Scheme 1. Schematic representation of SELEX

Scheme 1 shows the main steps of SELEX and how the procedure continues until a satisfactory set of oligonucleotides is obtained for a given ligand.

The conventional SELEX procedure has been used extensively over the years and provided outstanding results. For example, the applications in screening of thrombin aptamers²⁹, small molecule aptamers and VEGF aptamers³⁰ were noticeable in the recent past. Therefore, SELEX has revolutionized the field of molecular recognition by enabling the use of aptamers in a wide range of applications, from diagnostics to therapeutics and beyond.

1.3.1 Drawbacks of conventional SELEX

Despite the success of the SELEX procedure, there are several drawbacks that can limit its efficiency and applicability. For example, the SELEX procedure involves multiple rounds of selection, binding, partitioning, and amplification, which can be time-consuming. Typically, 8-15 rounds are necessary to achieve a high-affinity aptamer, which can take several weeks to complete.³¹ Apart from that, some targets such as membrane proteins or complex biological structures, may be difficult to access during SELEX. This limitation can result in the selection of aptamers with suboptimal binding characteristics. Also, the amplification of redundant sequences leads to a library that contains multiple copies of identical aptamers. This redundancy can reduce the overall diversity of the aptamer pool.

Moreover, the degradation by nuclease enzymes is a serious drawback of the aptamers screened by conventional SELEX.³² When it comes to live cells and conventional selection methodologies, they consist of multiple enzymatic steps. So, it is important to modify the aptamers to make them not susceptible for the enzymatic degradation.

When considering drawbacks, it is worth to mention that only a few aptamer-based medicines are in the clinical trials currently, while most of the designed medicines are in the early stage of development.³³ So far, only one drug has been approved by FDA, “Pegaptanib” in 2004, for the treatment of elderly macular disease.³⁴ Poor reproducibility,

low affinity and instability under required conditions have been identified as major limitations of developing aptamer-based medicines via SELEX. Therefore, it is essential to modify the aptamers in a suitable way to overcome the defects and to improve their performance.

There are several approaches to optimize the performance of aptamers. Modified SELEX methods such as IP-SELEX, Capture SELEX, Cell SELEX and CE-SELEX are some of the modifications of conventional SELEX.³⁵ IP SELEX consists of an additional step of immunoprecipitation (IP) to attract the targets in their native form. Usually, in in-vitro methods, the actual 3D structure of the targets is distorted. Hence the affinity of the aptamer is decreased under in-vitro conditions as the structure differs. But in this method, due to the IP step, the number of aptamers which are having the chance of recognizing the targets in usual physiological conditions can be increased. Consequently, the target specificity of the aptamer is increased.

In capture SELEX, the immobilization of the target is not required. Instead, oligonucleotide library is immobilized on a support. This method is developed to screen the aptamers against small soluble molecules.

Cell-SELEX is mostly used to screen aptamers for cancer cell targets. Live cells are used in the process and highly selective aptamers can be selected. Apart from that, CE-SELEX includes a capillary electrophoresis step, where the separation of ions is based on their electrophoretic mobility. This requires only a few rounds on selection to generate highly selective aptamers.

These are advanced methods, and their application could be limited to the selected procedure. However, general modifications which can be performed after the SELEX methods are usually more convenient and can be applied in different trajectories. These are called post-SELEX modifications.

1.4 Post-SELEX modifications

Any modification that is performed after the SELEX process is known as a post-SELEX modification. While SELEX is effective in identifying aptamers that bind to a variety of targets, the initial aptamers obtained from SELEX often require further modifications to improve their stability, binding affinity, specificity, and overall functionality. Therefore,

well planned post-SELEX modifications can overcome the limitations in conventional SELEX.

Depending on the method of modification, there are several categories of post-SELEX modifications, which will be explained below in detail. These modifications are widely applied practically in diagnostics, therapeutics and biotechnology.³⁶⁻³⁹

1.4.1 Chemical Modifications

Modifications can be introduced at different sites of the nucleotides. Basically, base modification, sugar group modification and backbone modification can be done according to the required optimization.⁴⁰ The nucleobase modifications are carried out by the replacement or alteration of an existing base of the nucleotide. For example, click chemistry reactions⁴¹ and binding with C5 of the pyrimidine bases⁴² are some of the nucleobase modifications that have been examined extensively in past research. The expected outcome of these modifications was increased binding affinity, specificity and selectivity. Figure 3 below represents two possible chemical modifications.

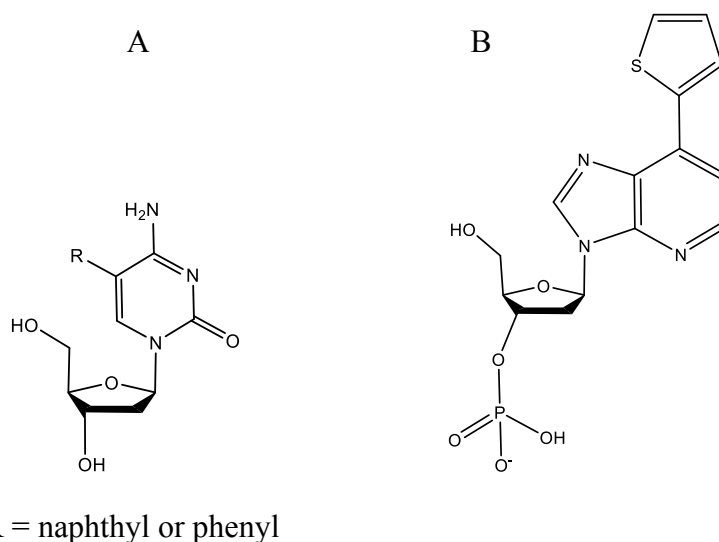


Figure 3. Chemical modifications performed as A) binding with C5 of pyrimidine base. B) Click chemistry reactions.

When considering sugar modifications, methyl substitutions and NH₂ substitutions for the 2' position of sugar group are widely used.⁴³ Apart from that, TNA

can be considered as another example for sugar modification, where five-carbon sugar group is replaced by a four-carbon sugar group. Previous studies reported that TNA was resistant to nuclease digestion which enhanced their thermal stability.⁴⁴ Figure 4 shows some of the modifications performed for sugar group.

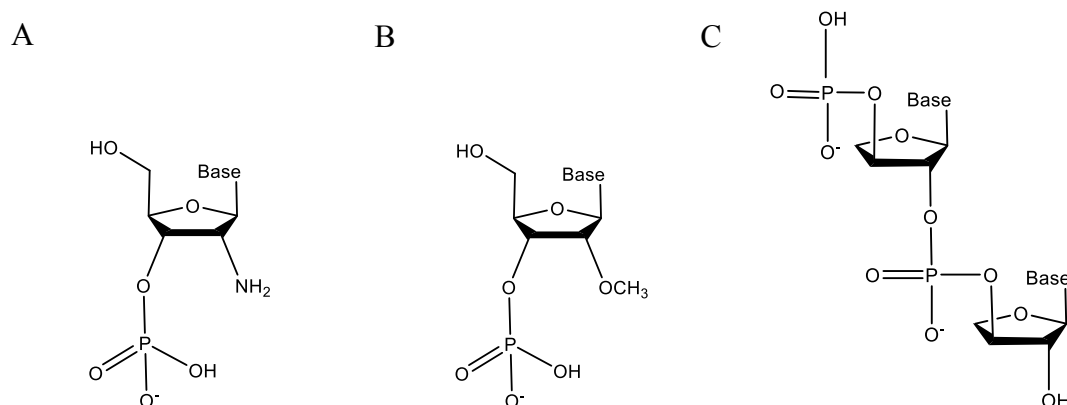


Figure 4. Modifications performed on the sugar group. A) Replacement of OH at 2' by NH₂ group. B) Replacement of OH at 2' by OCH₃ group. C) TNA: A four-carbon sugar group instead of five-carbon sugar.

LNAs are also a modification on sugar group where a connection is made between 2' oxygen atom and the C4 carbon of the sugar ring. In this way, the rigidity has been enhanced by hindering the free movement of the atoms. Also, the LNA modification increases the stability and resistance to nucleases.⁴⁵

Backbone modifications are another chemical modification, of which the preparation of phosphorothioate linkages provides an example. In this method, substitution of a non-bridging oxygen in the phosphate backbone with sulfur improves resistance to nuclease degradation. This approach is widely used in antisense oligonucleotides.⁴⁶ Moreover, peptide nucleic acid (PNA) is another backbone modification, where the backbone that is linked by peptide bonds instead of phosphodiester bonds. This modification decreases nuclease degradation of the aptamers as reported.⁴⁷ However, neutrally charged backbone in PNAs significantly deviates the binding properties of them compared to the conventional DNA/RNA aptamers. So due to the possible deviations resulted to the neutrality due to the difficulties in in-vitro selection process PNAs are not considered as a separate group of aptamers.

1.4.2. Truncation and optimization

Other than the chemical modifications, there are some alterations that can enhance the specificity of the aptamers. One approach is to reduce the length of aptamers by removing non-essential regions. Since the key binding sites still remain constant after truncation, these modifications can improve the aptamer's binding properties and reduce synthesis costs.⁴⁸ However, truncation does not always work as expected. Some works have reported that removing nonspecific regions has not improved the binding affinity. Hence, they emphasize that predicting the secondary structure and analyzing the binding mechanisms prior to the truncation improves the affinity of the aptamer. This can be done by molecular docking.⁴⁹

1.4.3. Limitations of post-SELEX modifications

Even though post-SELEX modifications have shown superior achievements that cannot be obtained by using only the conventional SELEX, there are certain limitations as well. For example, manufacturing issues such as scale up limitations are also possible with the modifications. Since the aptamer synthesis needs consistent quality control, it may be difficult to adhere to the optimum levels of product quality after some modifications.

When performing modifications, the selected aptamers are subjected to a whole new route of synthesis to obtain the desired modification. Any modification carried out after the initial selection of aptamers will increase the cost and time of the synthesis. Also, the complexity of the work is increased according to the degree of modifications that needs to be followed in the synthesis.

Other than the cost issues, the most important drawback is the loss of specificity and binding affinity after the alterations. For example, modifications to the nucleotide sequence or backbone of aptamers can sometimes disrupt the three-dimensional structure critical for binding to the target. This can lead to a reduction in binding affinity or specificity. Moreover, finding the right balance of modifications that enhance stability and functionality without assessing the binding properties can be difficult. Therefore, selection of truncations, removal or addition of new groups needs to be examined carefully.

Some modifications might introduce new points of instability. For example, phosphorothioate linkages, while enhancing nuclease resistance, can sometimes make the aptamer more prone to chemical degradation under physiological conditions. Apart from that, introduction of new groups may kick off unintended reactions such as interaction with intercellular proteins and cell surface.⁵⁰ This will potentially lead to non-specific binding and reduced overall effectiveness.

Biological incompatibility is another important concern. Alterations may cause a change in pharmacokinetics of the aptamers, affecting the distribution, metabolism and excretion of the compound and sometimes leading to adverse effects.

In general, while post-SELEX modifications play a vital role in expanding the effective usage of aptamers, it should be noted that the possibility of drawbacks also exists. So, in practise, a pre-assessment would be beneficial to avoid possible side reactions that could occur when performing the modifications.

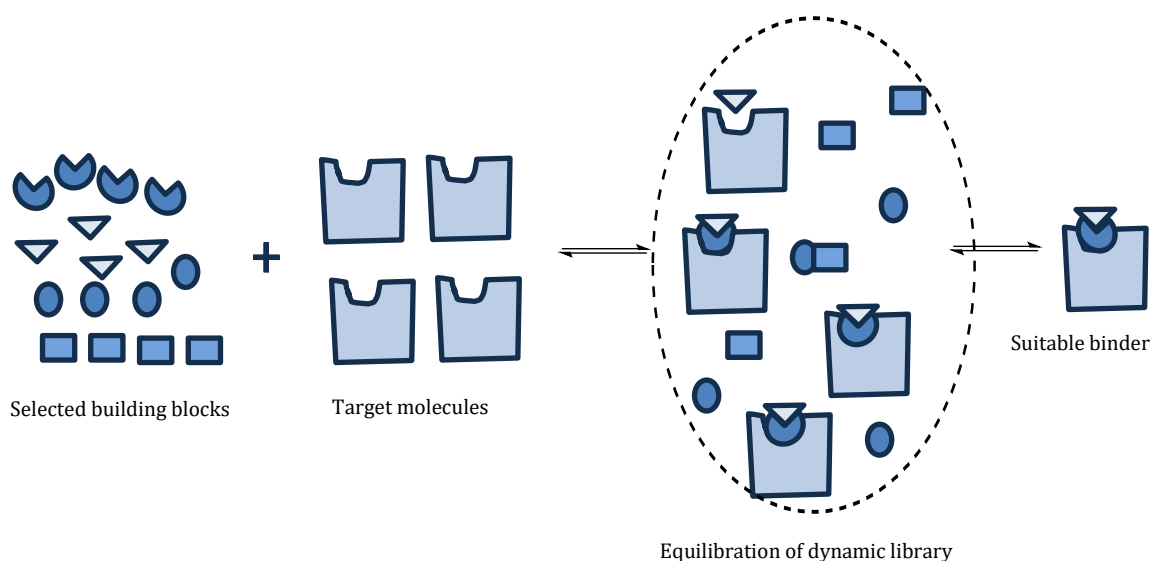
1.5 Dynamic Combinatorial Chemistry

1.5.1 General principles of DCC

Dynamic combinatorial chemistry (DCC) is an innovative approach in the field of chemical synthesis and molecular discovery. DCC is based on the thermodynamic equilibrium between the starting materials and products. There could be numerous different compounds in the pool of starting materials and each of them continuously react and interconvert through a reversible reaction. Basically, two different starting materials with different functional groups will be needed to react with each other reversibly. For example, aldehydes and amines can be reacted to form a dynamic combinatorial library of imines (Schiff bases). The reversibility of the starting materials and products makes DCC different from the conventional combinatorial chemistry. This can be addressed as a self-assembly process which can respond to changing conditions of the system, such as pH, temperature or other potential stimuli.⁵¹ However, these changes should not prevent the DCC reaction or cause any side reactions.⁵²

Scheme 2 below represents a schematic diagram of DCC. When the characterization is performed after the equilibrium reaction, the desired combination

could be identified and then these combinations can be isolated and purified by suitable methods.



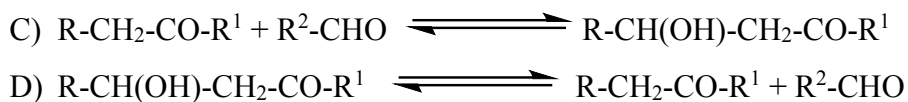
Scheme 2. Schematic representation of DCC.

When performing DCC, the dynamic libraries of interconverting components form reversible bonds under thermodynamic control. The presence of a target molecule stabilizes the best-binding compounds, shifting the equilibrium to favor their formation. The isolation and further handling of any component in its pure form requires another set of conditions that prevent any exchange reactions of the compound.⁵³ Therefore, it is important to not only consider the required conditions in the equilibrium but also for the conditions of stable best binders.

1.5.2 Coupling reactions

There are numerous reactions that can be considered as examples for the coupling reactions. Having different combinations of two functional groups of the starting materials will give rise to different combinations of products. Scheme 3 below shows some important coupling reactions used in DCC.





Scheme 3. Some of the important coupling reactions. A) Imine exchange. B) Disulfide exchange. C) Aldol reaction. D) Retroaldol reaction.

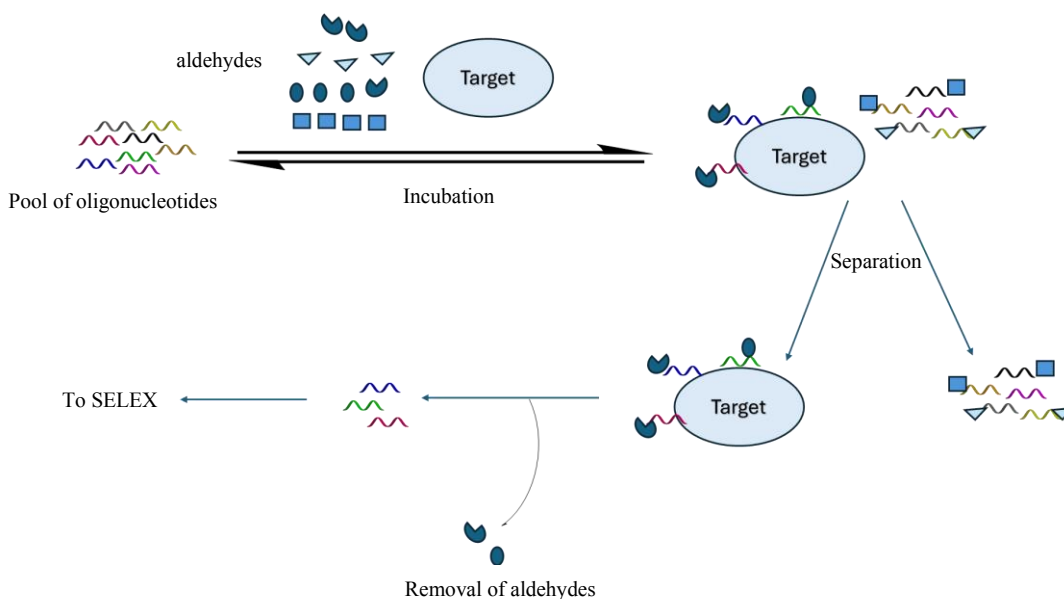
1.5.3 Applications of DCC

The generation of DCC libraries can be achieved through covalent or non-covalent binding of the components.⁵⁴ The use of transition metal coordination is one example of covalent binding which has been successfully employed.⁵⁵ Addition-elimination reactions at carbonyl groups such as imine exchange, transacetalization and aldol—retroaldol reactions are some of the reactions applicable in DCC. By changing the electronic properties of the carbonyl compound and the nucleophile, the reaction kinetics can be changed in a predictable way.⁵⁴ Also in these reversible mechanisms, the “freezing” of exchange conditions is performed by an external factor such as pH, catalysts, quenching reagents such as reduction/oxidation reagents or temperature.

In imine exchange reactions, the formation of imine is reversible. However, when it is converted into a secondary amine, the reaction will be “frozen”. This is achieved by introducing a reducing agent such as NaBH₃CN. Acid-base quenching can be observed in trans-acetalization reactions, where a suitable neutralizing agent stops the reversible mechanism. For example, if the reaction is catalyzed by acid, then addition of a base will stop the reaction. Moreover, for aldol and retroaldol reactions, the reaction can be frozen by addition of acids to adjust the pH. This will freeze the aldol product by neutralizing the base. In these ways, the binding composition will be stabilized, and the isolation of the composition will be easy.

Even though most of the reported applications of DCC are in protein binding,⁵⁶ there are significant applications in nucleic acid chemistry as well. Specially, when DCC is combined with SELEX, the dynamic diversity can increase the likelihood of identifying high-affinity aptamers. On the other hand, a dynamic combinatorial library can be introduced to the target molecule, as a pre-enrichment step before SELEX as shown in scheme 4. This will lead the molecule to bind with relevant binders to some extent even

before SELEX. During the actual SELEX, further optimization can be done to the aptamers.



Scheme 4. Schematic diagram of combination of DCC with SELEX

1.6 1,3-Oxazinanes and their reactions

1,3-oxazinanes are six-membered ring compounds where a nitrogen and oxygen are at positions 1 and 3.⁵⁷ Having several modifiable sites, they are significant in designing pharmacological structures. There are several FDA approved drugs such as Dirithromycin, Efavirenz and Dolutegravir which are 1,3-oxazinane derivatives.⁵⁸ These compounds have been studied significantly in recent years.

Recent works of our group have investigated the formation of nucleoside analogues of 1,3-oxazinane, namely *N*-methoxy-1,3-oxazinane nucleic acids (MOANA) which can be used in post-synthetic modification of oligonucleotides.⁵⁹ By reacting (2*R*,3*S*)-4-(methoxyamino)butane-1,2,3-triol with different types of aldehydes, different MOANA analogues were synthesized where the equilibrium depends on the pH and temperature. To obtain the dynamic combinatorial library, the reaction must reach the equilibrium and the best binders should be isolated by stopping the reaction. Altering the pH towards neutrality and maintaining the temperature below room temperature will “freeze” the reaction.

The reversible reaction mechanism of interconverting modified oligonucleotide scaffolds into MOANA analogues can be used as a foundation in many other synthetic

Scheme 6. Incorporation of nucleoside analogues to hairpin oligonucleotides. X denotes the modified site while R represents the rest of the aldehyde, except the aldehyde functional group.

1.7 Purpose of the research project

The plan was to design a dynamic combinatorial method to screen for high-affinity modified aptamers for quinine. The derivatization is performed by reacting the modified aptamers (T19, C20 and A21) with a pool of selected aldehydes separately at a suitable pH of 5.5 to the respective modified MOANA—DNA aptamer. The success depends on how the selected aldehydes are bound with the aptamer scaffold and how the resulting modified MOANA—DNA aptamers can bind to the target ligand. Other than that, maintaining a constant pH and temperature are important in this project.

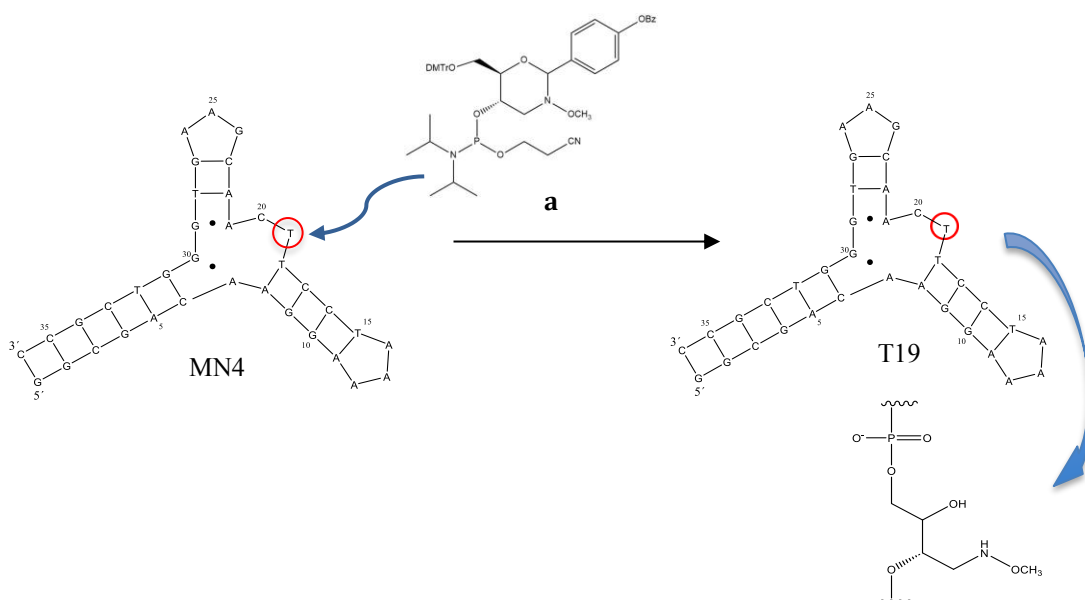
In this research project, the reversible reaction of modified aptamers and expected nucleoside analogues was controlled by pH, where the N-methoxy-1,3-oxazinane formation is preferred in pH 5.5. So, the reversible reaction will take place until it reaches the equilibrium to result a DCL of various binding complexes. The selected set of aldehydes demonstrated the role of suitable binding agents, with quinine as the target molecule.

In this project, quinine is used as the target ligand, instead of cocaine. Out of different structures of quinine, MN4 aptamer could be considered as a reasonable model to determine the binding affinity with target ligands. Therefore, the base sequence of MN4 is used, which consist of 36 nucleobases.

Binding of the introduced aldehydes is characterized by UHPLC-MS to identify the effective modifications and a logical comparison is made between how these modifications behave in the presence and absence of quinine. The aim was to identify the scaffold—aldehyde combinations with the highest binding affinity for quinine. For a quantitative analysis, the identified scaffolds are subjected to isothermal titration calorimetry.

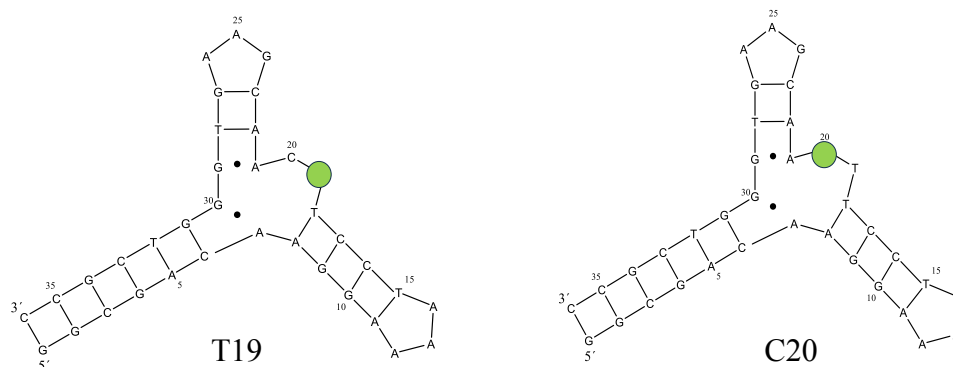
2 Results and Discussion

2.1 Oligonucleotide Synthesis



Scheme 7. Synthesis of T19 modified aptamer by the incorporation of benzylidene protected (2*R*,3*S*)-4-(methoxyamino)butane-1,2,3-triol phosphoramidite building block (a)

The sequence of MN4 aptamer was used as the preliminary sequence for the synthesis. The bases at positions 19, 20 and 21 were replaced one at a time by the previously synthesized 4-(benzoyloxy)benzylidene protected (2*R*,3*S*)-4-(methoxyamino)butane-1,2,3-triol phosphoramidite building block (MOANA residue). Hence, three different oligonucleotides (ONs) were synthesized and named according to the replaced base and its position. Figure 5 shows the 2D structure and Table 1 the base sequence of the three different modified aptamers synthesized.



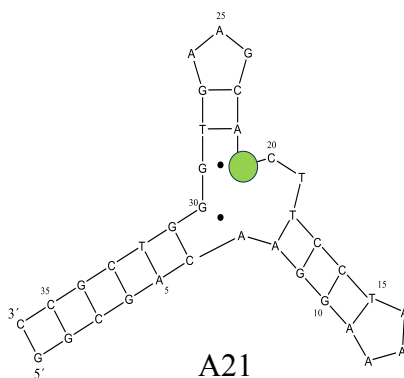


Figure 5. 2D structures of the modified aptamers. The green circle indicates the modified site.

Table 1. Sequences of modified aptamers. X denotes the MOANA residue.

Aptamer	Base sequence
MN4	5'-GGCGACAAGGAAAATCCTTCAACGAAGTGGGTCGCC-3'
T19	5'-GGCGACAAGGAAAATCCTXCAACGAAGTGGGTCGCC-3'
C20	5'-GGCGACAAGGAAAATCCTTXAACGAAGTGGGTCGCC-3'
A21	5'-GGCGACAAGGAAAATCCTTCXACGAAGTGGGTCGCC-3'

For all the three modified aptamers, the trityl response was monitored throughout the synthesis. Even though the synthesis of other nucleotides showed a typical near quantitative yield, a low response was observed at the modified sites for all the three aptamers. At the modified sites, the responses for the relative coupling percentages were 90.3%, 90.9% and 91.2% for the aptamers T19, C20 and A21 respectively. This indicated that the yields were relatively low for the modified aptamers. It was evident that the low yield might not be sufficient for the ITC studies planned for the latter part of the project. However, for a UPLC-MS analysis, the yields were adequate.

2.1.1 Purification of the modified aptamers

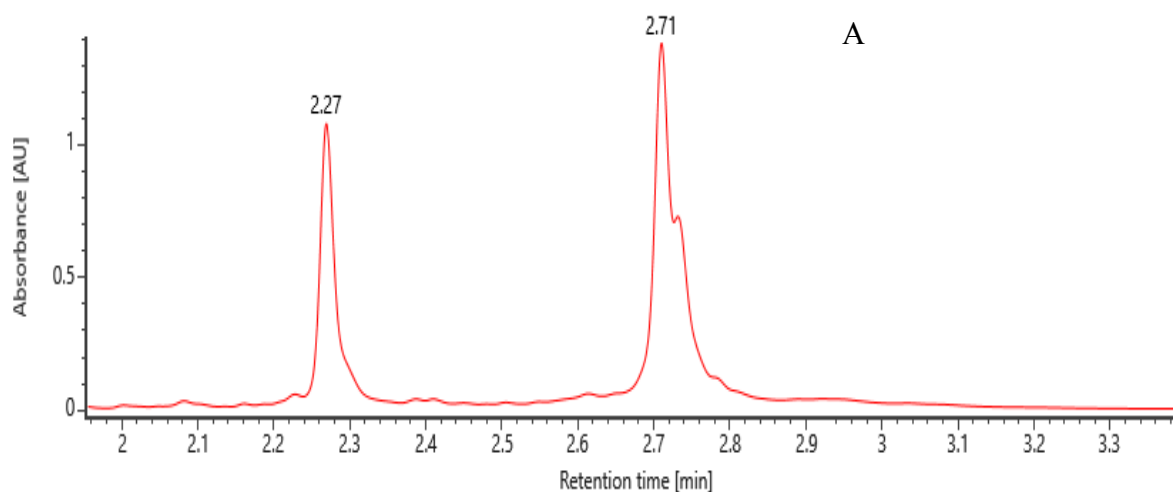
In the first attempt at purification of modified aptamer **T19**, a co-eluting peak was observed along with the desired peak. Alteration of the solvent programme did not resolve this issue and characterization through UHPLC-MS confirmed this co-eluting peak at 1802.9 m/z. Meanwhile, the intensity of the modified **T19** peak had decreased drastically

compared to the impurity peaks after several purifications. However, $^1\text{H-NMR}$ and $^{31}\text{P-NMR}$ spectra of the modified phosphoramidite building block confirmed that the compound was stable and not degraded. By considering all the details, it was decided to resynthesize the **T19** aptamer.

During the resynthesis, extra attention was given to the dryness of the phosphoramidite. Accordingly, it was dried by coevaporation from toluene which had a moisture content of 24.2 ppm (determined by Karl Fischer titration). The commercially available amidites were dried under a vacuum over phosphorus pentoxide. The trityl response at the modified site in the second synthesis was higher than in the previous synthesis but still relatively low.

The LC-MS analysis of this resynthesized T19 aptamer still showed the co-eluting peak along with the desired peak. Figure 6A shows the UHPLC spectrum of the crude **T19** which shows as a shoulder on the peak eluting at 2.71 min.

The issue of coeluting peaks was resolved by reacting **T19** with a hydrophobic aldehyde (cyclohexane carboxaldehyde) at pH 5.5. By this approach, an equilibrium was established between aldehyde bound form (N-methoxy-1,3-oxazinanone analogue) and unbound form with T19 when changing the pH values. Then the desired peak could be recovered in the aldehyde-bound form. Figure 6B shows the UHPLC profile of crude aldehyde-bound **T19** aptamer, with a new peak observed at 3.15 min.



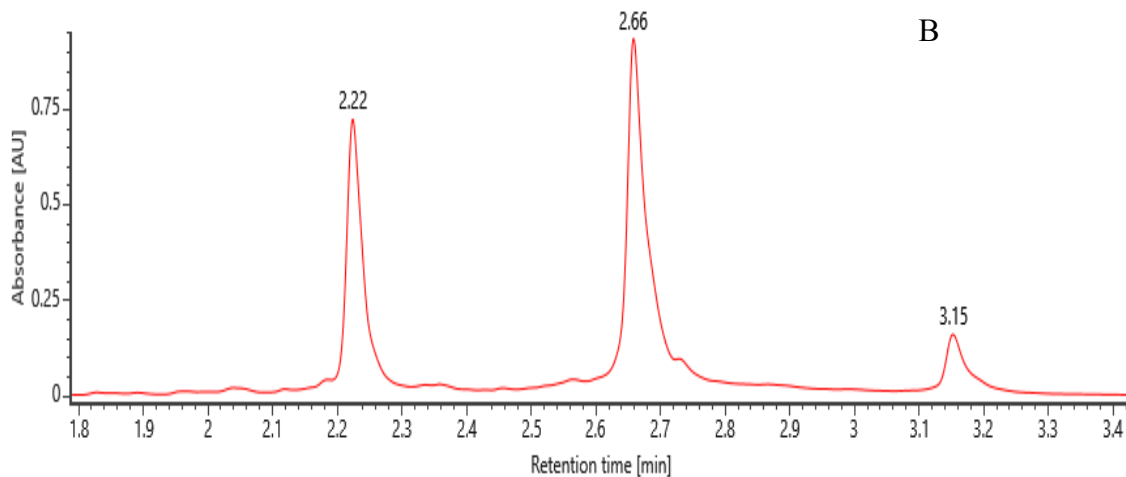


Figure 6. A) UHPLC profile of crude **T19**. **B)** UHPLC profile of **T19** + cyclohexane carboxaldehyde reaction at pH 5.5. H₂O, 40 mM HFIP, 7 mM TEA: H₂O, MeOH, 20 mM HFIP, 3.5 mM TEA (9:1v/v)

Mass spectrometric analysis of the peak eluted at 2.71 min in UHPLC profile in figure 6A showed that there are two prominent peaks. One of the peaks represents the product which formed by missing the modified building block from the sequence at 1802.94 m/z. and the other peak was the modified **T19** product at 1838.47 m/z in Figure 7.

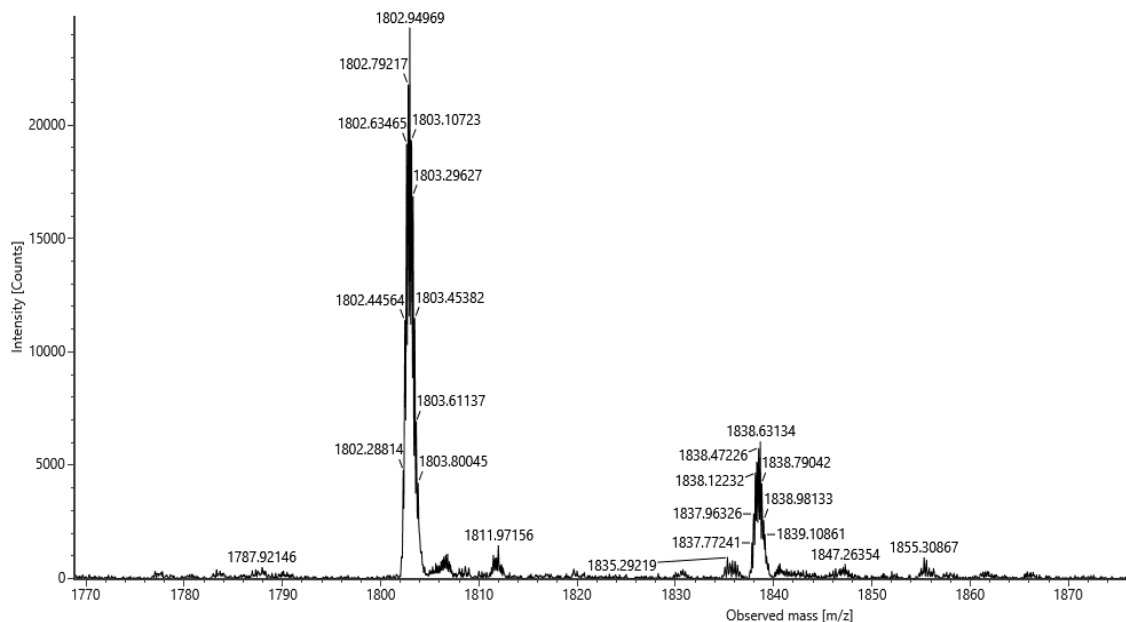


Figure 7. Mass spectrum of the peak eluting at 2.71 min.

In the mass spectrum for the UHPLC profile given in figure 6B, a new peak was detected at $m/z = 1854$ (pentaanion), This corresponds to the expected product of aldehyde-bound form which is represented in Figure 8 below.

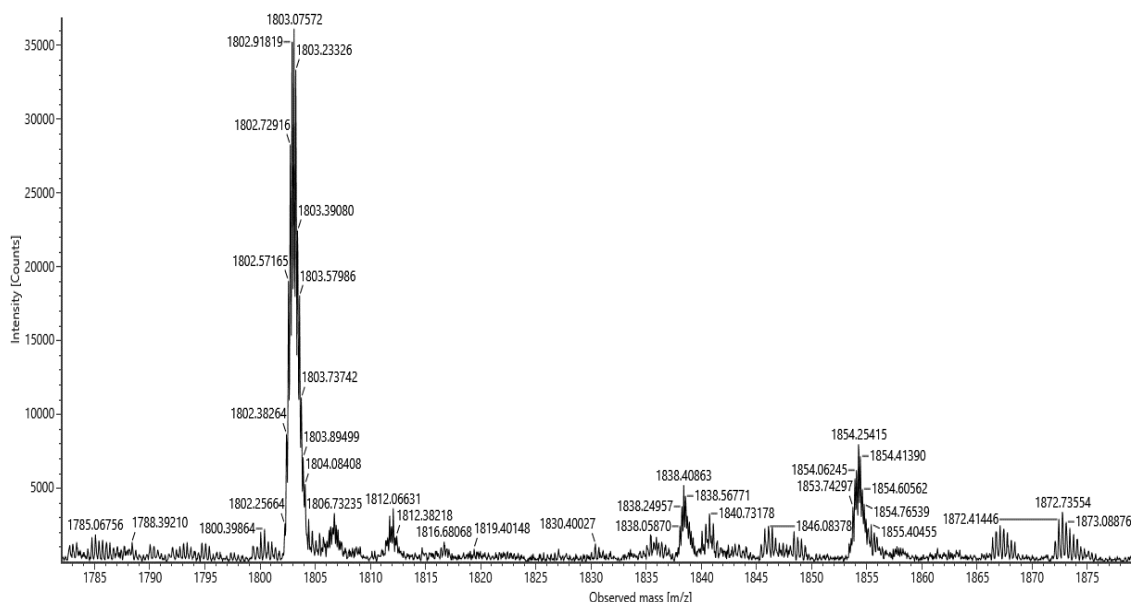


Figure 8. Mass spectrum of the **T19** + cyclohexane carboxaldehyde reaction mixture.

After three rounds of purification, the desired N-methoxy-1,3-oxazinanone analogue was isolated in a higher purity as shown in the UHPLC spectrum Figure 9 below. The peak at 3.04 min corresponds to the desired aldehyde-bound **T19** and the peak at 2.57 min represents the naked **T19** with no aldehyde bound. The other peak found at 2.68 min was assumed to be the 35mer product of the aptamer based on the calculated molecular weight and m/z values.

Figure 10 shows the relevant mass spectrum for the given UHPLC profile in figure 9. The peaks observed at 2.57, 2.68 and 3.04 in UHPLC profile in figure 9 are corresponded to the peaks at 1838.2 m/z , 1842.6 m/z and 1854.1 m/z in the figure 10 respectively. Detection of 1854 m/z at a considerable intensity confirmed the success of this approach.

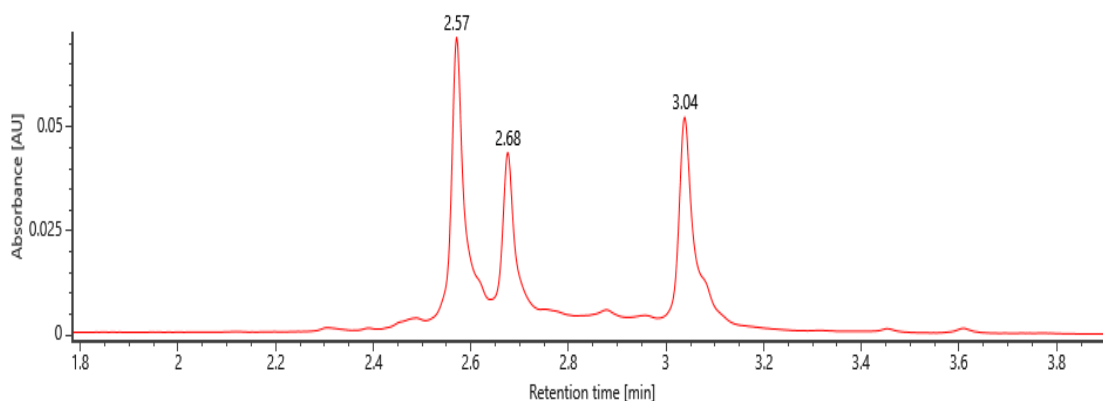


Figure 9. UHPLC profile of purified **T19** + cyclohexane carboxaldehyde at pH 5.5. H₂O, 40 mM HFIP, 7 mM TEA: H₂O, MeOH, 20 mM HFIP, 3.5 mM TEA (9:1v/v)

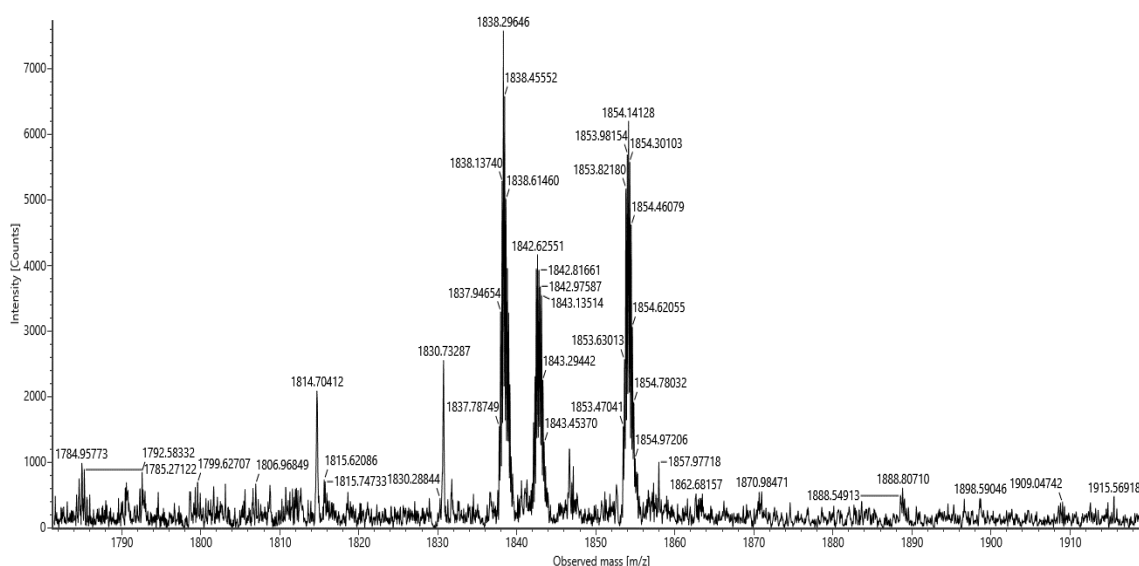


Figure 10. UHPLC-MS spectrum of purified **T19** + cyclohexane carboxaldehyde.

Similarly, the other two modified aptamers were also reacted with cyclohexane carboxaldehyde before the purification by RP-HPLC. The UHPLC spectra of **C20** and **A21** modified aptamers with aldehyde treatment were found to be satisfactory as the aldehyde bound peak eluted separately. Hence this aldehyde binding was a good approach to overcome the issue of co-eluting peaks. Figure 11 below clearly shows the desired peaks of aldehyde derivatized **C20** and **A21** aptamers without co-elution at 3.09 minute and 3.07 minute respectively.

After purification of all the three modified aptamers, the lyophilized samples were each dissolved in 100 μ l of milli-Q water and the concentrations were determined by UV

spectrophotometry. The concentrations were 52.75 μM , 63.5 μM and 28.85 μM for **T19**, **C20** and **A21** respectively.

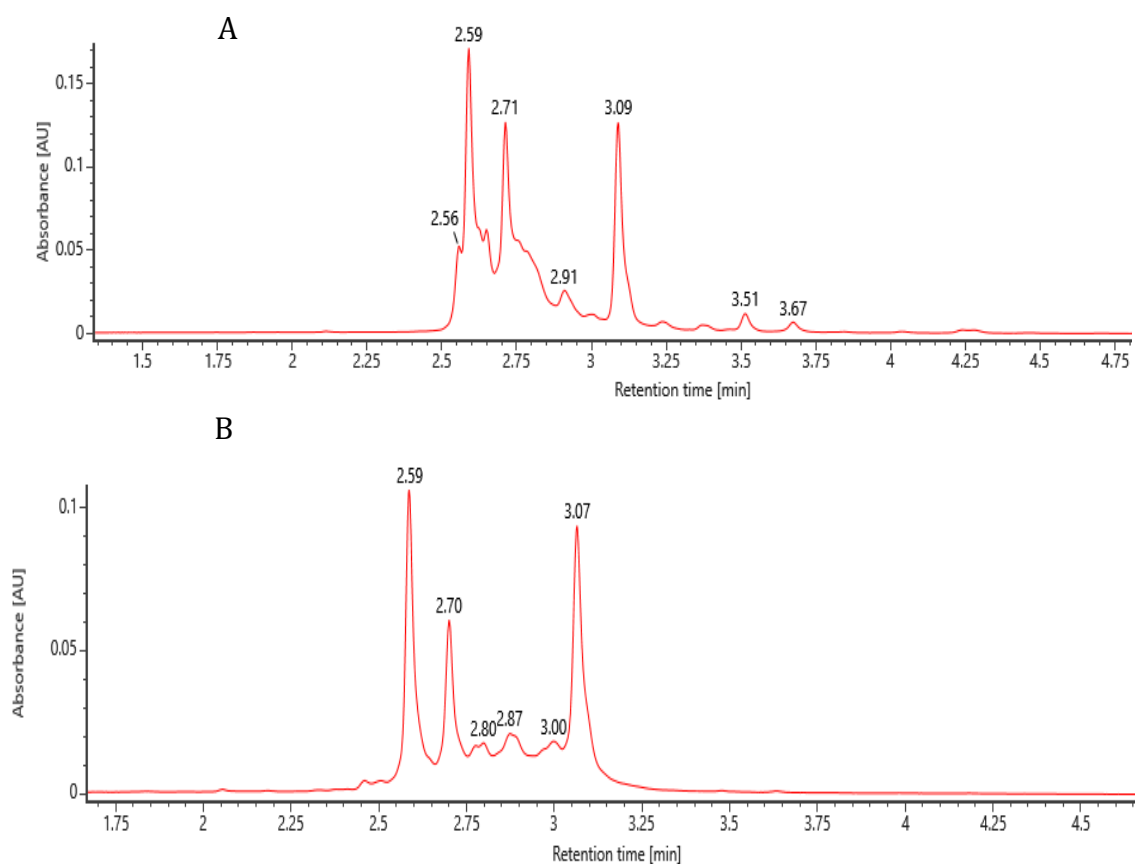


Figure 11. UHPLC spectrum of A) purified **C20** + cyclohexane carboxaldehyde reaction mixture, B) Purified **A21** + cyclohexane carboxaldehyde H_2O , 40 mM HFIP, 7 mM TEA: H_2O , MeOH, 20 mM HFIP, 3.5 mM TEA (9:1 v/v)

2.2 Selection of aldehydes for the DCC experiments

The modified aptamer scaffolds were derivatized by various aldehydes to investigate the impact on binding affinity with quinine. The selection of aldehydes was vital rather than selecting them randomly. Therefore, the structure of the aldehydes (aromatic and aliphatic nature) and the electronic distribution were considered when selecting the aldehydes, The aldehydes used in this project are summarized below in Table 2.

Group 1 aldehydes included acetaldehyde derivatives of nucleobases and some other heterocycles. Studies carried out on the incorporation of some nucleobase analogues to some of the hairpin oligonucleotides demonstrated promising binding affinities with

the selected oligonucleotides. Since the used nucleobase analogues in those studies are similar to the chemical structure of the DNA nucleobases, it was logical to observe the binding affinity of the four DNA nucleobases with the modified aptamer. However, binding of these aldehydes was not efficient except for the adenine derivative.

Aldehydes in group 2 included a combination of aliphatic, aromatic and cyclic aldehydes. When considering these aldehydes, an attention was given to the simple chemical structure. It consists of simple structured aldehydes which are not sterically crowded. Also, the reactivity and the polarity of these aldehydes were different from each other. Having different functional groups at different positions of the aliphatic chain changes the polarity of the molecules from one another. To examine the binding affinity of an aromatic aldehyde, benzyloxypropionaldehyde was also introduced to the group. All these variations were introduced to make the group more diversified, so it will be easy to get clear conclusions on how the modified aptamer scaffolds tend to bind with these different aldehydes.

The group 3 aldehydes were carefully selected benzaldehyde derivatives. Since the electronic distribution around the molecule changes according to the attached group, the Hammett constant values (σ) of these aldehydes were considered. The aldehydes which had similar σ values ($-\sigma$ or $+\sigma$) were reacted at a time, based on the attached ED groups or EW groups.

Benzaldehyde and 4-carboxybenzaldehyde are almost similar in σ values. So, it was logical to test those two together. However, no prominent binding was observed with these two aldehydes. Apart from that, 4-hydroxybenzaldehyde and 4-methoxybenzaldehyde contain electron donating groups. The reactivity of the aldehyde group is expected to be increased in these two aldehydes, hence the binding with the modified aptamer was expected to be promising. Surprisingly, there was no binding observed in either occasion. The final combination was methyl-4-formylbenzoate and 3-nitrobenzaldehyde which have positive σ values. Due to the presence of electron withdrawing groups, the reactivity could be lower than with the other aldehydes used. Therefore, the DCC equilibrium reaction was expected to be slow in this combination. However, most effective bindings were observed with these two aldehydes, despite the low reactivity. Table 3 indicates the σ values of the aldehydes.

Table 2. Selected aldehydes and the groups of them based on the selection.

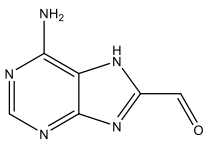
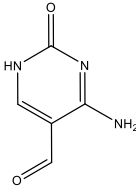
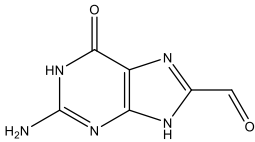
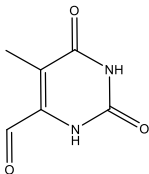
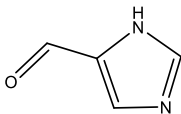
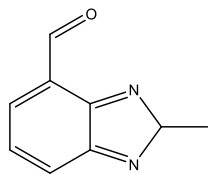
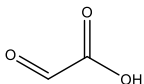
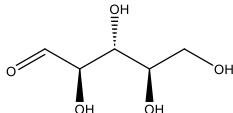
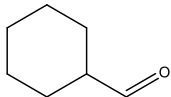
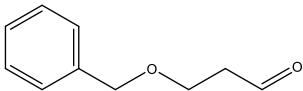
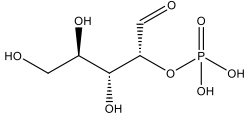
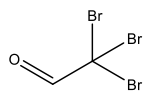
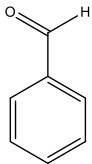
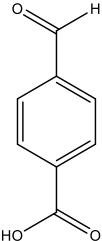
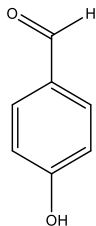
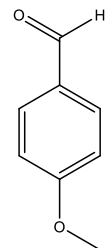
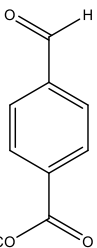
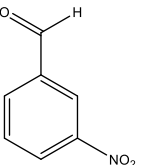
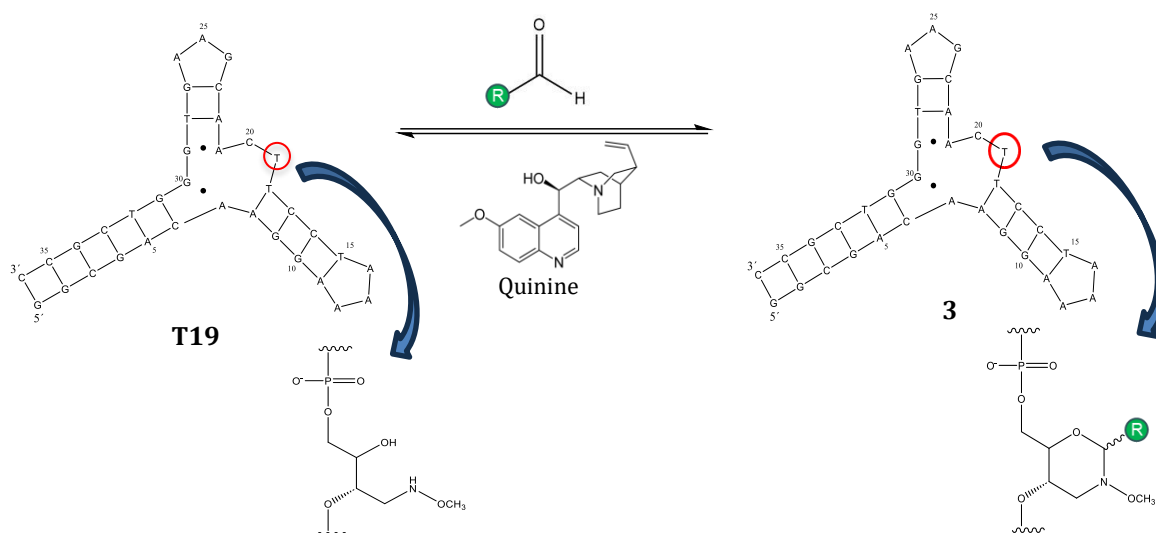
Group	Aldehyde			
1				
	Adenine (G1a)	Cytosine (G1b)	Guanine (G1c)	
				
	Thymine (G1d)	Imidazole (G1e)	2-methylbenzimidazole (G1f)	
	2			
		Glyoxylic acid (G2a)	Cyclohexanecarbaldehyde (G2b)	D-ribose (G2c)
				
Benzylpropylaldehyde (G2d)		D-ribose monophosphate (G2e)	Tribromoacetaldehyde (G2f)	
3				
		Benzaldehyde (A1a)	4-carboxybenzaldehyde (A1b)	4-hydroxybenzaldehyde (A2a)
				
	4-methoxybenzaldehyde (A2b)	methyl-4-formylbenzoate (A3a)	3-nitrobenzaldehyde (A3b)	

Table 3. Hammett substituent constants (σ) for the aldehydes in group 3

Aldehyde	Hammett constant value (σ)
4-carboxybenzaldehyde	-0.05
Benzaldehyde	0
4-hydroxybenzaldehyde	-0.38
4-methoxybenzaldehyde	-0.28
methyl-4-formylbenzoate	+0.39
3-nitrobenzaldehyde	+0.55

2.3 Derivatization of modified aptamers with aldehydes



Scheme 8. Derivatization of modified aptamer **T19** with aldehydes at pH 5.5 and room temperature to obtain N-methoxy-1,3-oxazinanone analogues (**3**) in the presence of quinine. The “R” group bound to the MOANA analogue represents the rest of the aldehyde, except the aldehyde functional group.

Scheme 8 shows the formation of a MOANA analogue of the **T19** aptamer. Similarly, other two MOANA analogues of **C20** and **A21** aptamers were synthesized by the same process mentioned above. Here the scheme represents the reaction in the presence of quinine. However, another reaction was performed in the absence of quinine by keeping all the other conditions and reagents unchanged.

In the UHPLC-MS analysis of the reaction mixtures, intensities of the penta-anion signals of the aptamer scaffolds and their various MOANA derivatives were compared. The calculated values for the scaffold-aldehyde combinations were assessed to confirm the product formation, both in the presence and the absence of quinine. Moreover, the relative intensities of other products were also observed to compare the formation of such products.

Out of the tested aptamer scaffolds, **A21** had no considerable binding with any of the aldehydes, in either presence or absence of quinine. The mass spectra of **T19** and **C20** aptamers with group 1 aldehyde mixtures indicated conjugation with adenine aldehyde in both the presence and absence of quinine. It was observed that in the presence of quinine, this conjugation was less favoured than in the absence thereof. Apart from adenine, there was no conjugation observed in group 1 aldehydes with any of the modified aptamers. None of the data interpreted a clear impact on the binding affinity for quinine with any of the aldehydes in group 1.

Mass spectra of the aptamer scaffolds incubated in the group 2 aldehyde mixture clearly indicated that the conjugations of the aldehydes were not successful in either the presence or the absence of quinine. The unbound (naked) form of the aptamer was more prominent than the conjugated form with any of the aldehydes in group 2. In other words, the aldehydes in group 2 were more reluctant to bind with the aptamer scaffolds than the group 1 aldehydes. Out of the 6 aldehydes in group 2, only benzyloxypropionaldehyde showed significant conjugation with **T19** and **C20** in the absence of quinine. No appreciable conjugation was observed with **A21** regardless of the presence of quinine.

Consequently, when considering failures in group 1 and group 2, it can be assumed that the binding affinity of quinine is much higher on the respective binding sites than the aldehydes in group 1 and group 2. This may hinder the binding site before the derivatization with aldehydes or else the binding of quinine may fold the aptamer into a conformation where it is unfavourable to reach the aldehydes to react. Therefore, in the presence of quinine, the reversible reaction is more favoured towards the left side.

In the 3rd group of aldehydes, the A1 and A2 subsets gave similar results as the group 2 aldehydes, with little binding in either of the reaction mixtures. The naked aptamer, formaldehyde and acetaldehyde derivatives were observed in higher intensities

in both absence and presence of quinine. Therefore, these derivatizations were not useful to examine the impact on the quinine binding affinity.

Out of all the aldehydes studied, methyl-4-formylbenzoate and 3-nitrobenzaldehyde were the two aldehydes showing a significant response to the presence of quinine. These two aldehydes conjugated well with **C20**, both in the presence and absence of quinine. But it was observed that the conjugation with methyl-4-formylbenzoate was considerably efficient. In figure 12, the pentaanion peak of $m/z = 2238.56$ indicates the methyl-4-formylbenzoate derivative while $m/z = 2235.75$ indicates the 3-nitrobenzaldehyde derivative. The ratio of the two peaks is bit more higher than 2:1 which confirms the conjugation of methyl-4-formylbenzoate was more efficient in the presence of quinine.

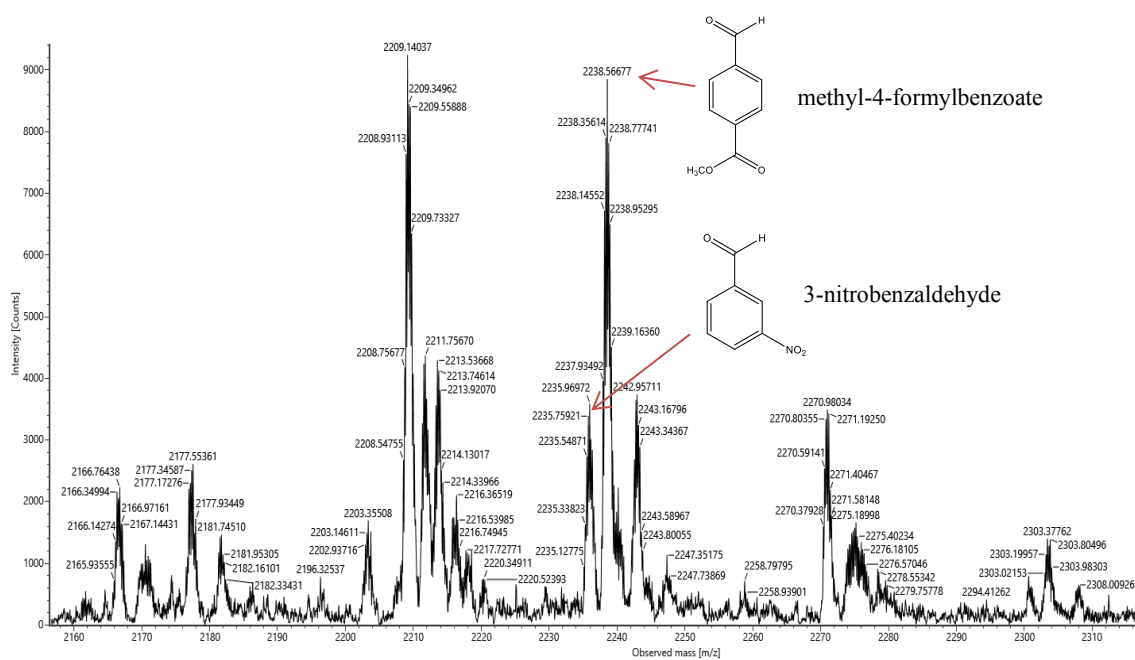


Figure 12. Mass spectra of C20 with A3 aldehyde mixture in the presence of quinine.

In the absence of quinine, the conjugation of 3-nitrobenzaldehyde was significantly increased while little change was observed with methyl-4-formylbenzoate, as shown in Figure 13. Simultaneously, the intensity of the peak corresponding to the naked aptamer dropped drastically. Now the intensities of the peaks of methyl-4-formylbenzoate at 2238.5 m/z and 3-nitrobenzaldehyde at 2235.7 m/z have a ratio of 1:1 which shows the increased conjugation in the absence of quinine. Derivatization with methyl-4-formylbenzoate did not limit the binding of quinine, hence it showed a proper binding in

both absence and presence of quinine. Apart from that, the conjugation with 3-nitrobenzaldehyde was more efficient in the absence of quinine. This observation suggests that the quinine might hinder the binding region of aptamer. Consequently, out of all the aldehydes tested, the conjugation of methyl-4-formylbenzoate and 3-nitrobenzaldehyde were prominent as they showed a considerable reactivity difference in the presence and absence of quinine. Therefore, these two scaffold-aldehyde combinations can be further used in aptamer screening methods.

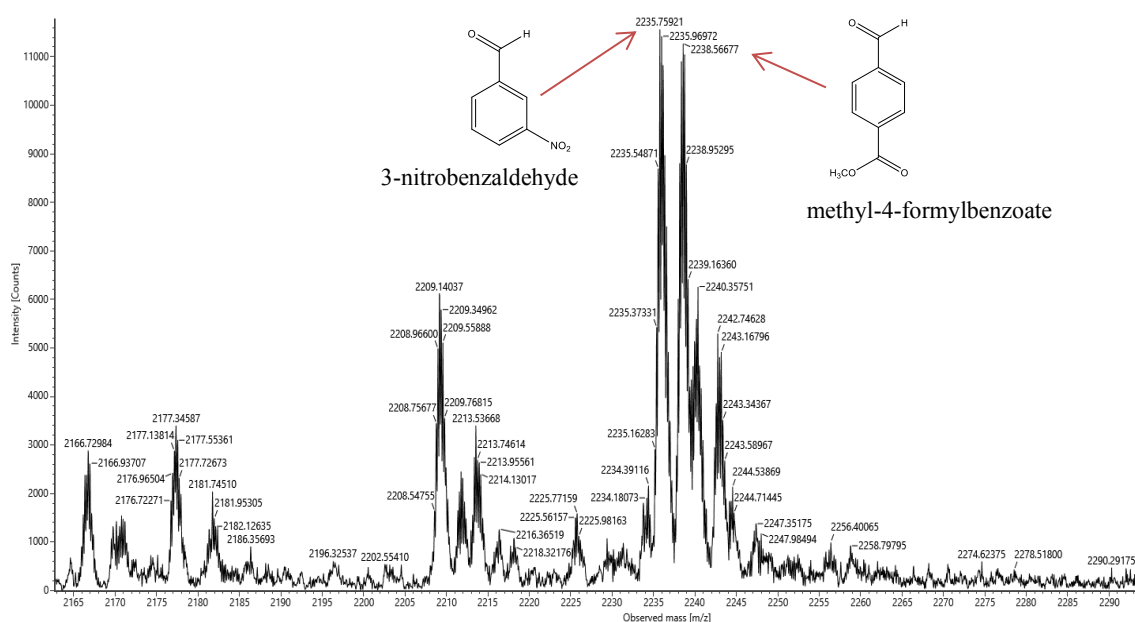


Figure 13. Mass spectra of C20 with A3 aldehyde mixture in the absence of quinine.

An interesting result was observed with the group 3 aldehydes, when they reacted with T19 in the presence of quinine. Instead of the expected naked aptamer peak of 2206.0 m/z, a peak at 2200.3 m/z was observed, as indicated in Figure 14. This was observed most prominently for the T19 aptamer in the presence of quinine. It was assumed to be a product of the N-O bond cleavage since the 2200.3 peak is a perfect match for the loss of OCH₃ group from T19. Since this was only observed in the presence of quinine, it is interesting to study further the involvement of quinine and the how the position within the aptamer drives this reaction forward.

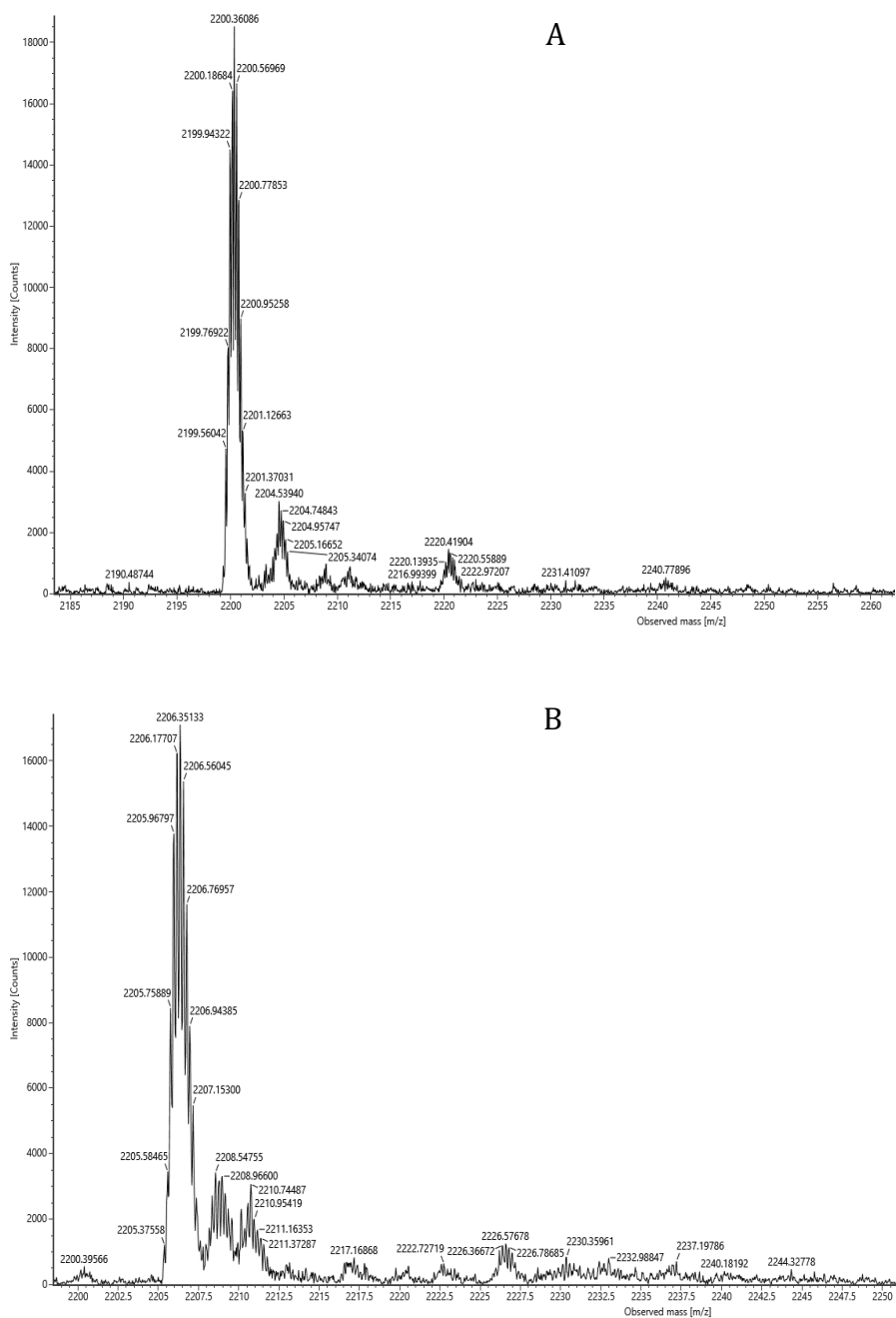


Figure 14. Mass spectra of **T19** with A1 aldehyde mixture. A) in the presence of quinine. B) in the absence of quinine.

2.4 Isothermal Titration Calorimetric studies

The initial plan of the project was to identify scaffold-aldehyde combinations with a high binding affinity towards quinine by UHPLC-MS. The binding constants, enthalpy and entropy would then be quantified by ITC. Based on the UHPLC-MS results, methyl-4-

formylbenzoate and 3-nitrobenzaldehyde were selected for the ITC analysis since they showed a considerable difference of reactivity in the presence and absence of quinine when they conjugate with **C20**. Prior to the analysis, two aldehydes were reacted separately with the **C20** aptamer in the same buffer as used for the DCC studies. The reaction progress was monitored by UHPLC-MS until it reached equilibrium and then the crude products were purified by RP-HPLC by using the same solvent system as before. The purification must ensure that there are no other components which could bind with quinine in the ITC studies.

In ITC studies, the aptamer concentration and the titrant concentration should be selected carefully. It has been reported that the titrant concentration should be around 15-20 times higher than the aptamer concentration. However, in this research project, the limiting factor was the concentration of the aptamer, which was more than 3 times lower than the sensitivity of the ITC instrument.

The concentration range of the modified aptamer in previous related studies has been 10 – 20 μM . The specifications of the instrument available (MicroCal iTC200), on the other hand, mentioned that the lowest concentration that can be used is 3 μM . However, the concentrations of the aptamer-aldehyde conjugates of methyl-4-formylbenzoate and 3-nitrobenzaldehyde were 0.83 μM and 0.96 μM respectively, insufficient for a clear signal in ITC. Therefore, the ITC studies were not successful during this project.

3 Experimental

3.1 General methods and materials

Commercially available solvents and reagents were used in the syntheses. Toluene was dried over 4 Å molecular sieves and the moisture content was checked by Karl Fischer titration. The mass spectra were recorded by Waters ACQUITY RDa mass spectrometer. Quantifications of the synthesized aptamers were performed by Shimadzu UV 1900 UV-Vis spectrophotometer. Shimadzu VP HPLC system with LC-10AT pump and UV detector was used for the purifications. 50 mM TEAA in milli-Q water and 50 mM TEAA in ACN were used as the HPLC solvents.

3.2 Synthesis of modified aptamers

Three modified aptamer scaffolds (**T19**, **C20**, and **A21**) were synthesized by incorporating the previously synthesized⁵⁹ 4-benzoyloxybenzylidene protected (2R,3S)-4-(methoxyamino)butane-1,2,3-triol phosphoramidite building block into various positions within the known cocaine aptamer **MN4**. The name of the modified aptamer was given according to the position of replaced nucleotide. Three aptamer scaffolds were synthesized separately by replacing the phosphoramidite building block with the pre-determined position by one at a time. Prior to each synthesis, appropriate amount of the phosphoramidite was dissolved in 25 ml of dried toluene and evaporated to dryness. This step was repeated three times to remove any residual moisture.

The commercially available amidites (dA, dT, dG and dC) and previously synthesized phosphoramidite building block(**a**) were weighed and kept in a vacuum desiccator over phosphorous pentoxide for a better dryness. Then they were dissolved completely in appropriate volumes of acetonitrile and loaded on the synthesizer. The ÄKTA oligopilot plus 10 DNA/RNA synthesizer was used to synthesize the modified aptamers in 1.0 μmol scale by using conventional phosphoramidite strategy and 20 mg of Ac-dc-CPG solid support was used inside the synthesis column for the synthesis. Trityl responses were monitored, and they revealed that the couplings at the modified sites for all the three modified aptamers were not efficient as expected. Because the coupling efficiencies and the detritylated areas for these modified sites showed lower values compared to the other couplings in the sequence. However, the final yields were reasonably adequate to carry out the procedure further.

After the synthesis, the synthesis column was detached from the synthesizer and the solid support transferred into a falcon tube. 2 ml of 25% aqueous NH_3 was added to the tube and the resulting heterogeneous mixture allowed to incubate for 4 h at 55 °C. After the NH_3 treatment, the liquid layer was separated carefully and freeze-dried. The freeze-dried sample was dissolved in 1 ml of milli-Q water and analyzed by Waters ACQUITY RDa mass spectrometer, before being purified by RP-HPLC. The UHPLC-MS results confirmed formation of the expected modified aptamers but also there were prominent impurity peaks which were originated from the truncation of the aptamer and from the product formed by modified nucleotide.

During the purification by RP-HPLC, it was observed that the expected peak for the modified aptamer co-eluted with another peak, which was difficult to separate from each other. To facilitate separation, the modified aptamers were derivatized with a hydrophobic aldehyde. To perform this reaction, a 0.1 M solution of cyclohexane carboxaldehyde was first prepared in DMSO. 100 μ l (10 μ mol) of this solution was mixed with 1 ml of modified aptamer solutions (**T19**, **C20** and **A21** separately). Then 25 μ l of 2 M TEAA buffer (pH 5.5) was added to each of the above mixtures. The reaction mixtures were incubated for 3 days and reaction progress was analyzed by UHPLC-MS by injecting a sample of 1:100 dilution with milli-Q water. UHPLC-MS analysis showed well separated desired peaks for all the 3 modified aptamers. The reaction mixtures were neutralized with a drop of triethylamine prior to the purification of RP-HPLC.

Crude aptamer scaffolds were purified by Shimadzu RP-HPLC on a bioZen 2.6 μ m oligo LC column (150 x 4.6 mm). The eluting gradient was 5 - 25% of CAN in 50 mM aqueous TEAA over 20 min and 25 - 5% over the next 5 min. The flow rate was kept at 0.6 ml/min and the detection wavelength was 260 nm.

Several rounds of purification were performed for each modified aptamer, until an acceptable purity was achieved. The collected fractions were characterized by UHPLC-MS and the desired m/z peaks were detected. After the purification, the three modified aptamer samples were freeze-dried and dissolved in 100 μ l of milli-Q water.

The purified aptamers were quantified by UV spectrophotometer under 260 nm and the concentrations were calculated by Oligo Calc online calculator.

3.3 Derivatization of modified aptamers with aldehydes

3.3.1 Preparation of aldehyde samples

5 mM solutions of each aldehyde in group 1 were prepared by dissolving them in DMSO or in water, depending on the aldehyde solubility. A portion of 8 μ l from each solution was withdrawn and mixed with 100 mM cacodylate buffer (20 ml, pH 5.5) to prepare a 2 μ M aldehyde mixture (G1). The same procedure was followed with the group 2 aldehydes and the mixture named as G2. For group 3 aldehydes, 2 μ M aldehyde mixtures (A1, A2 and A3) were prepared by mixing only two aldehydes at a time. Solution A1 was prepared by mixing 5 mM 4-carboxybenzaldehyde (8 μ l) and 5 mM benzaldehyde (8 μ l) stock solutions with 100 mM cacodylate buffer (20 ml). Similarly, A2 was prepared mixing 5

mM 4-hydroxybenzaldehyde (8 μ l) and 5 mM 4-methoxybenzaldehyde (8 μ l) stock solutions with 20 ml of 100 mM cacodylate buffer, while A3 was prepared by mixing 5 mM methyl-4-formylbenzoate (8 μ l) and 5 mM 3-nitrobenzaldehyde (8 μ l) stock solutions with 20 ml of 100 mM cacodylate buffer.

3.3.2 Incubation with aldehydes at pH 5.5

Incubation was performed at pH 5.5 and room temperature. To assess the impact of quinine, two sets of reaction mixtures were prepared – one with and one without quinine. 52.75 μ M (1.89 μ l, 100 pmol) **T19** aptamer (52.75 μ M) was mixed with 2 μ M of either G1, G2, A1, A2 and A3 aldehyde mixture (100 μ l, 200 pmol). 2 mM quinine sulphate dihydrate (10 μ l, 20 nmol) was added to each of these mixtures. Similarly, another set of reaction mixtures were prepared in the absence of quinine. Both reaction mixtures were allowed to reach equilibrium at room temperature and protected from light. The progress of the reaction mixtures was monitored over 2 weeks by analyzing samples at regular intervals by UHPLC-MS. Initially, the formation of the expected products was determined and after two weeks the relative intensities of the starting materials and the products were compared. If there is no significant change in the relative intensities of product formation, it was concluded that the reaction has reached to the equilibrium. The same procedure was carried out by reacting 63.5 μ M **C20** (1.57 μ l, 100 pmol) and 28.85 μ M **A21** (3.46 μ l, 100 pmol) separately with 2 μ M each of the aldehyde mixtures (100 μ l, 200 pmol) in the presence and absence of quinine.

3.4 Isothermal Titration Calorimetric studies

3.4.1 Preparation and purification of modified aptamers

After identifying the best candidates by DCC, they were prepared in larger scale for ITC analysis. 20 μ l (1.27 nmol) of **C20** and 5.5 μ l of 100 mM cacodylate buffer were added separately to 2.54 μ l of 5 mM methyl-4-formylbenzoate and to 2.54 μ l of 5 mM 3-nitrobenzaldehyde to prepare 20 mM solutions. The reaction mixtures were allowed to reach equilibrium and product formation was verified by UHPLC-MS. The mixtures were purified by the same procedure as described in section 3.3. The purified samples were analyzed by UHPLC-MS and confirmed the expected product in a reasonable purity. Purified samples were freeze-dried overnight. After freeze drying, the residue was

dissolved in 350 μ l of buffer (pH 7.4, 20 mM Tris•HCl, 140 mM NaCl, 5 mM KCl). Then aptamer concentration was determined by UV vis spectrometer.

3.4.2 ITC studies

The aldehyde-derivatized **C20** aptamer sample which was dissolved in 350 μ l of buffer was used as the titrand. 18 μ M quinine sulphate solution was prepared by dissolving an appropriate amount in the same buffer. ITC was performed by iTC200 microcalorimeter. Titration was carried out at 15 °C by placing the quinine as the titrant and the aptamer samples in the sample cell. The initial injection was 0.1 μ l and the standard binding experiments consisted of 35 successive 1 μ L injections at a spacing of 300 seconds between each injection. The data was analyzed by Origin 7.0 software.

4 Summary and Conclusion

The syntheses of modified aptamer scaffolds **T19**, **C20** and **A21** were successful despite the low-yielding. Derivatization of the aptamer scaffolds with a hydrophobic aldehyde proved to be an efficient method to overcome the issue of co-elution with shorter side products.

Out of the tested aldehydes, methyl-4-formylbenzoate and 3-nitrobenzaldehyde showed an efficient binding in both the presence and absence of quinine for the modified aptamer **C20**. Out of these two, the conjugation with methyl-4-formylbenzoate with the aptamer scaffold **C20** was considerably efficient in both the presence and absence of quinine. With the other aldehydes, the formation of N-methoxy-1,3-oxazinane analogues was more or less equal in the absence and presence of quinine which does not indicate an impact on the binding affinity of quinine.

Even though some promising aptamer—aldehyde conjugates were identified by UHPLC-MS, determination of their quinine binding constants by ITC was not successful owing to insufficient amounts.

Indication of an unexpected peak at 2200 m/z for **T19** with third group of aldehydes in the presence of quinine was assumed to be a N-O bond cleavage as it was a perfect match for a OCH₃ loss. This can be considered as a quinine-induced bond cleavage, since it appeared only in the presence of quinine.

In conclusion, two scaffold-aldehyde combinations were identified which has satisfactory level of affinity towards quinine. Methyl-4-formylbenzoate showed a better conjugation in both the presence and absence of quinine, while the conjugation of 3-nitrobenzaldehyde was more favored in the absence of quinine. Therefore, these two modified aptamer-aldehyde combinations can be further used in aptamer screening methods.

5 References

1. L. Hernandez, I. Machado, T. Schafer, F. Hernandez. Aptamers Overview: Selection, Features and Applications. *Curr Top Med Chem* **2015**, 15 (12), 1066–1081.
2. L.F. Yang, M. Ling, N. Kacherovsky, S.H. Pun. Aptamers 101: aptamer discovery and *in vitro* applications in biosensors and separations. *Chem Sci* **2023**, 14 (19), 4961–4978.
3. K.-M. Song, S. Lee, C. Ban. Aptamers and Their Biological Applications. *Sensors* **2012**, 12 (1), 612–631.
4. K. Han, Z. Liang, N. Zhou. Design Strategies for Aptamer-Based Biosensors. *Sensors* **2010**, 10 (5), 4541–4557.
5. J. Zhou, J. Rossi. Aptamers as targeted therapeutics: Current potential and challenges. *Nature Reviews Drug Discovery*. Nature Publishing Group March 1, 2017, pp 181–202.
6. S.M. Nimjee, R.R. White, R.C. Becker, B.A. Sullenger. Aptamers as Therapeutics. *Annu Rev Pharmacol Toxicol* **2017**, 57 (1), 61–79.
7. A.D. Keefe, S. Pai, A. Ellington. Aptamers as therapeutics. *Nat Rev Drug Discov* **2010**, 9 (7), 537–550.
8. E.W.M. Ng, D.T. Shima, P. Calias, et al. Pegaptanib, a targeted anti-VEGF aptamer for ocular vascular disease. *Nat Rev Drug Discov* **2006**, 5 (2), 123–132.
9. S. Deshpande, Y. Yang, S. Zauscher, A. Chilkoti. Enzymatic Synthesis of Aptamer-Polynucleotide Nanoparticles with High Anticancer Drug Loading for Targeted Delivery. *Biomacromolecules* **2024**, 25 (1), 155–164.
10. P. Parekh, S. Kamble, N. Zhao, et al. Immunotherapy of CD30-expressing lymphoma using a highly stable ssDNA aptamer. *Biomaterials* **2013**, 34 (35), 8909–8917.
11. J. Tan, N. Yang, Z. Hu, et al. Aptamer-Functionalized Fluorescent Silica Nanoparticles for Highly Sensitive Detection of Leukemia Cells. *Nanoscale Res Lett* **2016**, 11 (1), 298.

12. Z. Hu, J. Tan, Z. Lai, et al. Aptamer Combined with Fluorescent Silica Nanoparticles for Detection of Hepatoma Cells. *Nanoscale Res Lett* **2017**, 12 (1), 96.
13. E.J. Cho, J.-W. Lee, A.D. Ellington. Applications of Aptamers as Sensors. *Annual Review of Analytical Chemistry* **2009**, 2 (1), 241–264.
14. X. Chen, C. Zhou, X. Guo. Ultrasensitive Detection and Binding Mechanism of Cocaine in an Aptamer-based Single-molecule Device. *Chin J Chem* **2019**, 37 (9), 897–902.
15. V.I. Kukushkin, N.M. Ivanov, A.A. Novoseltseva, et al. Highly sensitive detection of influenza virus with SERS aptasensor. *PLoS One* **2019**, 14 (4), e0216247.
16. S.J. Lee, J. Cho, B.-H. Lee, D. Hwang, J.-W. Park. Design and Prediction of Aptamers Assisted by In Silico Methods. *Biomedicines* **2023**, 11 (2), 356.
17. A.N. Edwards, A.N. Iannucci, J. VanDenBerg, et al. G-Quadruplex Structure in the ATP-Binding DNA Aptamer Strongly Modulates Ligand Binding Activity. *ACS Omega* **2024**, 9 (12), 14343–14350.
18. M.N. Stojanovic, P. de Prada, D.W. Landry. Aptamer-Based Folding Fluorescent Sensor for Cocaine. *J Am Chem Soc* **2001**, 123 (21), 4928–4931.
19. X. Chen, C. Zhou, X. Guo. Ultrasensitive Detection and Binding Mechanism of Cocaine in an Aptamer-based Single-molecule Device. *Chin J Chem* **2019**, 37 (9), 897–902.
20. Z.-G. Wang, O.I. Wilner, I. Willner. Self-Assembly of Aptamer–Circular DNA Nanostructures for Controlled Biocatalysis. *Nano Lett* **2009**, 9 (12), 4098–4102.
21. A.A. Shoara, Z.R. Churcher, T.W.J. Steele, P.E. Johnson. Analysis of the role played by ligand-induced folding of the cocaine-binding aptamer in the photochrome aptamer switch assay. *Talanta* **2020**, 217, 121022.
22. M.A.D. Neves, O. Reinstein, P.E. Johnson. Defining a Stem Length-Dependent Binding Mechanism for the Cocaine-Binding Aptamer. A Combined NMR and Calorimetry Study. *Biochemistry* **2010**, 49 (39), 8478–8487.
23. O. Reinstein, M. Yoo, C. Han, et al. Quinine Binding by the Cocaine-Binding Aptamer. Thermodynamic and Hydrodynamic Analysis of High-Affinity Binding of an Off-Target Ligand. *Biochemistry* **2013**, 52 (48), 8652–8662.

24. S. Slavkovic, M. Altunisik, O. Reinstein, P.E. Johnson. Structure-affinity relationship of the cocaine-binding aptamer with quinine derivatives. *Bioorg Med Chem* **2015**, 23 (10), 2593–2597.
25. J. Bao, S.M. Krylova, O. Reinstein, P.E. Johnson, S.N. Krylov. Label-Free Solution-Based Kinetic Study of Aptamer–Small Molecule Interactions by Kinetic Capillary Electrophoresis with UV Detection Revealing How Kinetics Control Equilibrium. *Anal Chem* **2011**, 83 (22), 8387–8390.
26. R. Pei, A. Shen, M.J. Olah, et al. High-resolution cross-reactive array for alkaloids. *Chemical Communications* **2009**, No. 22, 3193.
27. A.A. Shoara, Z.R. Churcher, T.W.J. Steele, P.E. Johnson. Analysis of the role played by ligand-induced folding of the cocaine-binding aptamer in the photochrome aptamer switch assay. *Talanta* **2020**, 217.
28. C. Tuerk, L. Gold. Systematic Evolution of Ligands by Exponential Enrichment: RNA Ligands to Bacteriophage T4 DNA Polymerase. *Science (1979)* **1990**, 249 (4968), 505–510.
29. E.W.M. Ng, D.T. Shima, P. Calias, et al. Pegaptanib, a targeted anti-VEGF aptamer for ocular vascular disease. *Nat Rev Drug Discov* **2006**, 5 (2), 123–132.
30. X. Fang, W. Tan. Aptamers Generated from Cell-SELEX for Molecular Medicine: A Chemical Biology Approach. *Acc Chem Res* **2010**, 43 (1), 48–57.
31. M. Darmostuk, S. Rimpelova, H. Gbelcova, T. Ruml. Current approaches in SELEX: An update to aptamer selection technology. *Biotechnol Adv* **2015**, 33 (6), 1141–1161.
32. Y. Tabuchi, J. Yang, M. Taki. Relative Nuclease Resistance of a DNA Aptamer Covalently Conjugated to a Target Protein. *Int J Mol Sci* **2022**, 23 (14), 7778.
33. S. Devi, N. Sharma, T. Ahmed, et al. Aptamer-based diagnostic and therapeutic approaches in animals: Current potential and challenges. *Saudi J Biol Sci* **2021**, 28 (9), 5081–5093.
34. E.W.M. NG, A.P. ADAMIS. Anti-VEGF Aptamer (Pegaptanib) Therapy for Ocular Vascular Diseases. *Ann N Y Acad Sci* **2006**, 1082 (1), 151–171.
35. Y. Zhang, B.S. Lai, M. Juhas. Recent advances in aptamer discovery and applications. *Molecules* **2019**, 24 (5).

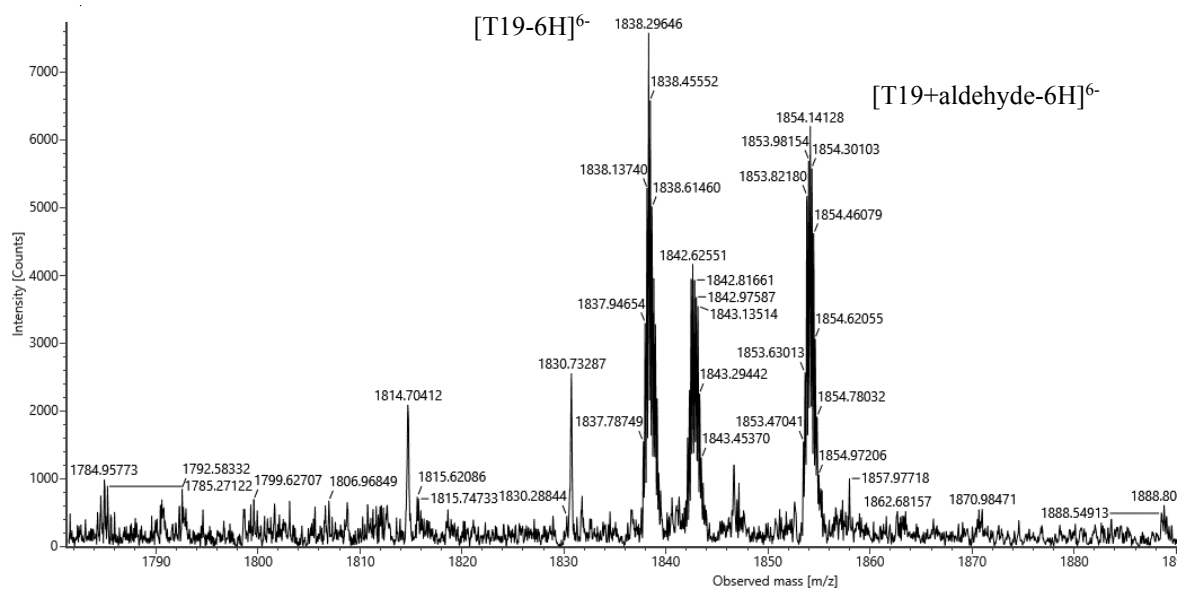
36. J.P. Elskens, J.M. Elskens, A. Madder. Chemical modification of aptamers for increased binding affinity in diagnostic applications: Current status and future prospects. *International Journal of Molecular Sciences*. MDPI AG June 1, 2020, pp 1–31.
37. S. Ni, H. Yao, L. Wang, et al. Chemical modifications of nucleic acid aptamers for therapeutic purposes. *International Journal of Molecular Sciences*. MDPI AG August 2, 2017.
38. D.-H. Kim, J.-M. Seo, K.-J. Shin, S.-G. Yang. Design and clinical developments of aptamer-drug conjugates for targeted cancer therapy. *Biomater Res* **2021**, 25 (1).
39. Y. Zhang, B.S. Lai, M. Juhas. Recent advances in aptamer discovery and applications. *Molecules* **2019**, 24 (5).
40. D. Ji, H. Feng, S.W. Liew, C.K. Kwok. Modified nucleic acid aptamers: development, characterization, and biological applications. *Trends Biotechnol* **2023**, 41 (11), 1360–1384.
41. M. Kovačič, P. Podbevšek, H. Tateishi-Karimata, et al. Thrombin binding aptamer G-quadruplex stabilized by pyrene-modified nucleotides. *Nucleic Acids Res* **2020**, 48 (7), 3975–3986.
42. X. Fan, L. Sun, Y. Wu, L. Zhang, Z. Yang. Bioactivity of 2'-deoxyinosine-incorporated aptamer AS1411. *Sci Rep* **2016**, 6, 25799.
43. C.L. Esposito, K. Van Roosbroeck, G. Santamaria, et al. Selection of a Nuclease-Resistant RNA Aptamer Targeting CD19. *Cancers (Basel)* **2021**, 13 (20), 5220.
44. M.R. Dunn, C.M. McCloskey, P. Buckley, K. Rhea, J.C. Chaput. Generating Biologically Stable TNA Aptamers that Function with High Affinity and Thermal Stability. *J Am Chem Soc* **2020**, 142 (17), 7721–7724.
45. D. Ji, H. Feng, S.W. Liew, C.K. Kwok. Modified nucleic acid aptamers: development, characterization, and biological applications. *Trends Biotechnol* **2023**, 41 (11), 1360–1384.
46. B.P. Monia, J.F. Johnston, H. Sasmor, L.L. Cummins. Nuclease Resistance and Antisense Activity of Modified Oligonucleotides Targeted to Ha-. *Journal of Biological Chemistry* **1996**, 271 (24), 14533–14540.
47. E.J. Lee, H.K. Lim, Y.S. Cho, S.S. Hah. Peptide nucleic acids are an additional class of aptamers. *RSC Adv* **2013**, 3 (17), 5828.

48. D. Shangguan, Z. Tang, P. Mallikaratchy, Z. Xiao, W. Tan. Optimization and Modifications of Aptamers Selected from Live Cancer Cell Lines. *ChemBioChem* **2007**, 8 (6), 603–606.
49. J. Nie, L. Yuan, K. Jin, et al. Electrochemical detection of tobramycin based on enzymes-assisted dual signal amplification by using a novel truncated aptamer with high affinity. *Biosens Bioelectron* **2018**, 122, 254–262.
50. J.H. Chan, S. Lim, W.F. Wong. ANTISENSE OLIGONUCLEOTIDES: FROM DESIGN TO THERAPEUTIC APPLICATION. *Clin Exp Pharmacol Physiol* **2006**, 33 (5–6), 533–540.
51. P. Frei, R. Hevey, B. Ernst. Dynamic Combinatorial Chemistry: A New Methodology Comes of Age. *Chemistry – A European Journal* **2019**, 25 (1), 60–73.
52. P.T. Corbett, J. Leclaire, L. Vial, et al. Dynamic Combinatorial Chemistry. *Chem Rev* **2006**, 106 (9), 3652–3711.
53. S. Otto, R.L.E. Furlan, J.K.M. Sanders. Dynamic combinatorial chemistry. *Drug Discov Today* **2002**, 7, 117–125.
54. O. Ramström, J.M. Lehn. Drug discovery by dynamic combinatorial libraries. *Nature Reviews Drug Discovery*. European Association for Cardio-Thoracic Surgery 2002, pp 26–36.
55. P.N.W. Baxter, J.-M. Lehn, K. Rissanen. Generation of an equilibrating collection of circular inorganic copper(i) architectures and solid-state stabilisation of the dicopper helicate component. *Chemical Communications* **1997**, No. 14, 1323–1324.
56. R. Huang, I. Leung. Protein-Directed Dynamic Combinatorial Chemistry: A Guide to Protein Ligand and Inhibitor Discovery. *Molecules* **2016**, 21 (7), 910.
57. K. Yang, F. Bi, J. Zhang, et al. Comparative research on promising energetic 1,3-diazinane and 1,3-oxazinane structures. *Arabian Journal of Chemistry* **2022**, 15 (7), 103947.
58. M.D. Delost, D.T. Smith, B.J. Anderson, J.T. Njardarson. From Oxiranes to Oligomers: Architectures of U.S. FDA Approved Pharmaceuticals Containing Oxygen Heterocycles. *J Med Chem* **2018**, 61 (24), 10996–11020.

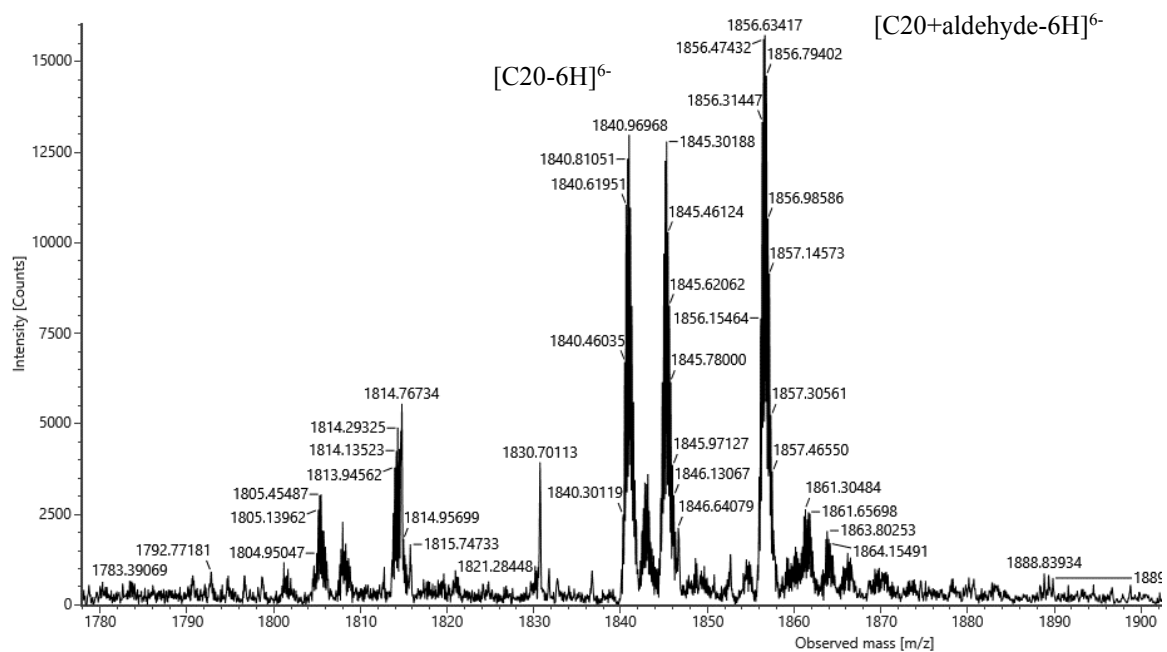
59. J. Wallin, T. Lönnberg. Improved Synthesis Strategy for *N*-Methoxy-1,3-oxazinane Nucleic Acids (MOANAs). *European J Org Chem* **2022**, 2022 (35).
60. M.N.K. Afari, K. Nurmi, P. Virta, T. Lönnberg. Watson-Crick Base Pairing of *N*-Methoxy-1,3-Oxazinane (MOANA) Nucleoside Analogues within Double-Helical DNA. *ChemistryOpen* **2023**, 12 (7).

6 Appendices

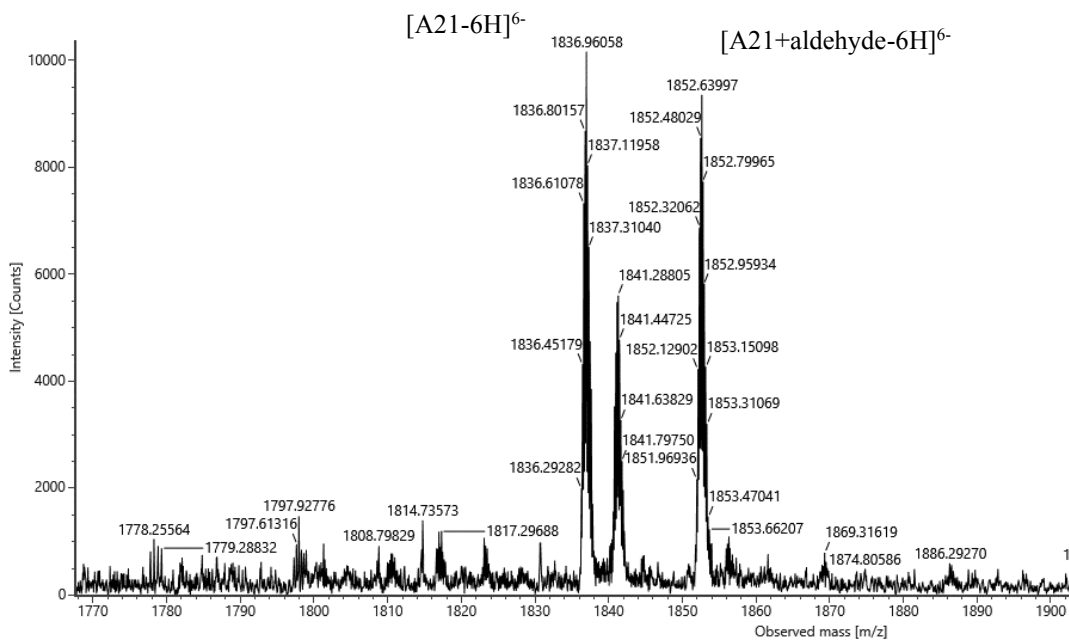
Appendix 1: Mass spectrum of purified **T19** after the cyclohexane carbaldehyde treatment.



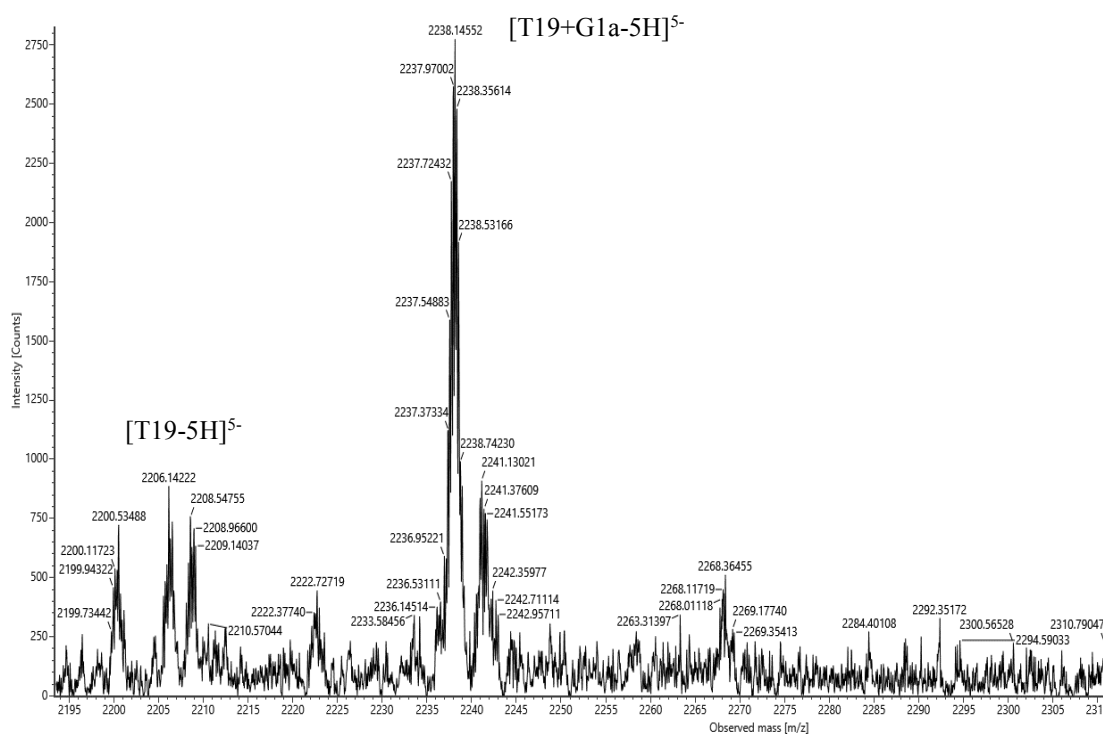
Appendix 2: Mass spectrum of purified **C20** after the cyclohexane carbaldehyde treatment.



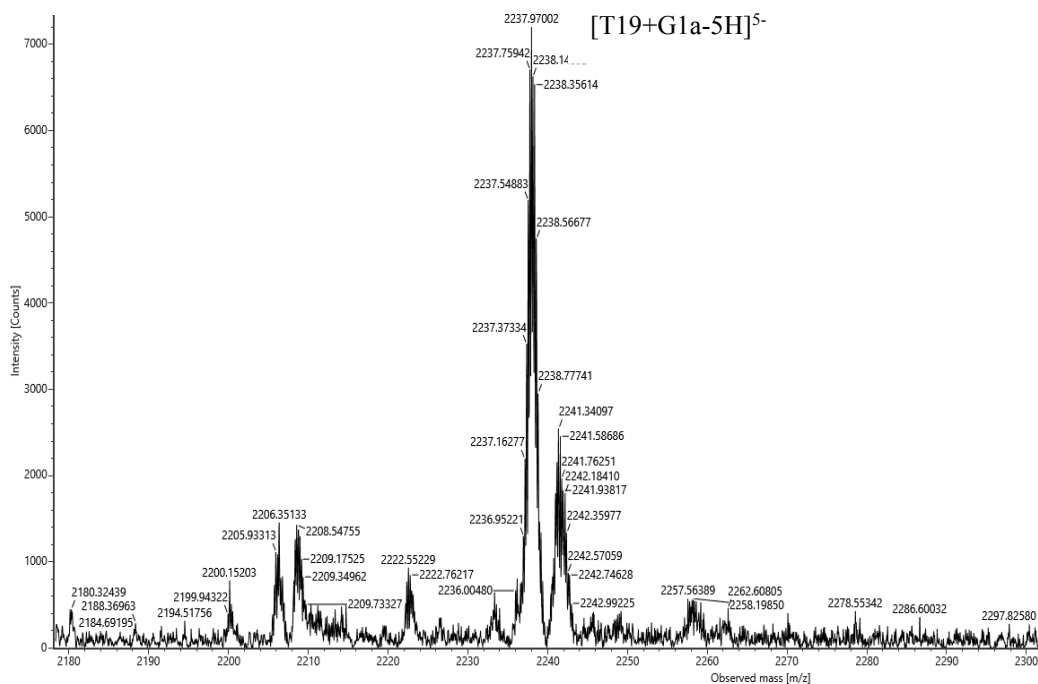
Appendix 3: Mass spectrum of purified **A21** after the cyclohexane carbaldehyde treatment.



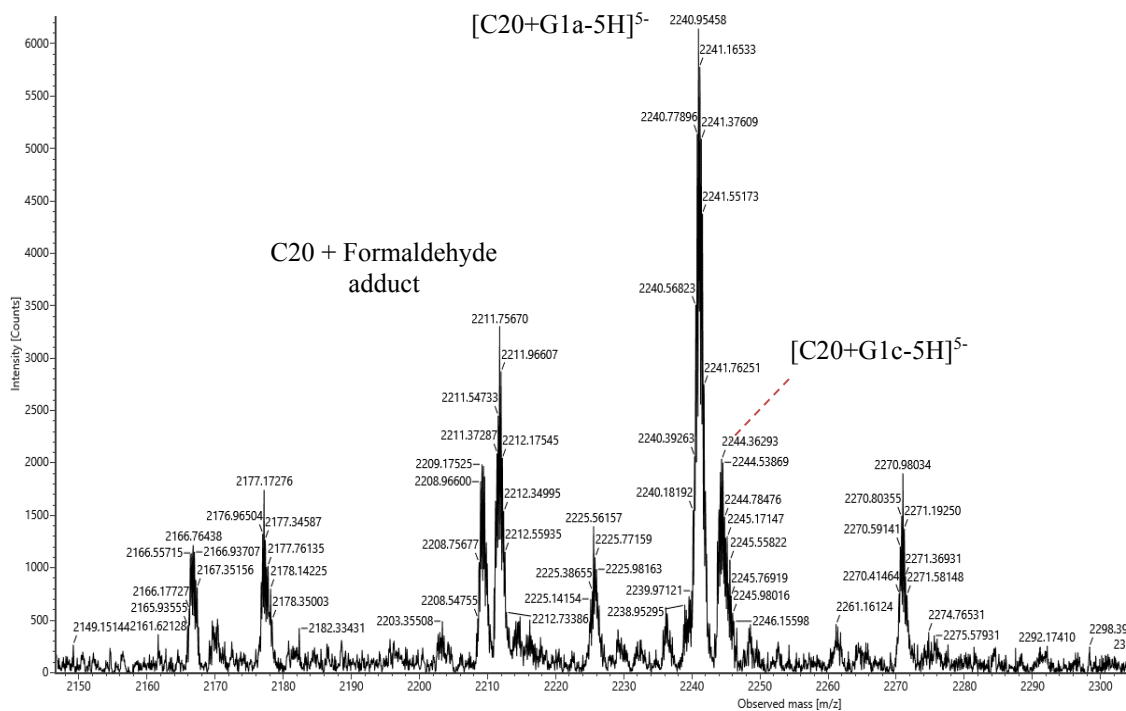
Appendix 4: Mass spectrum of **T19** with G1 aldehyde set in the presence of quinine.



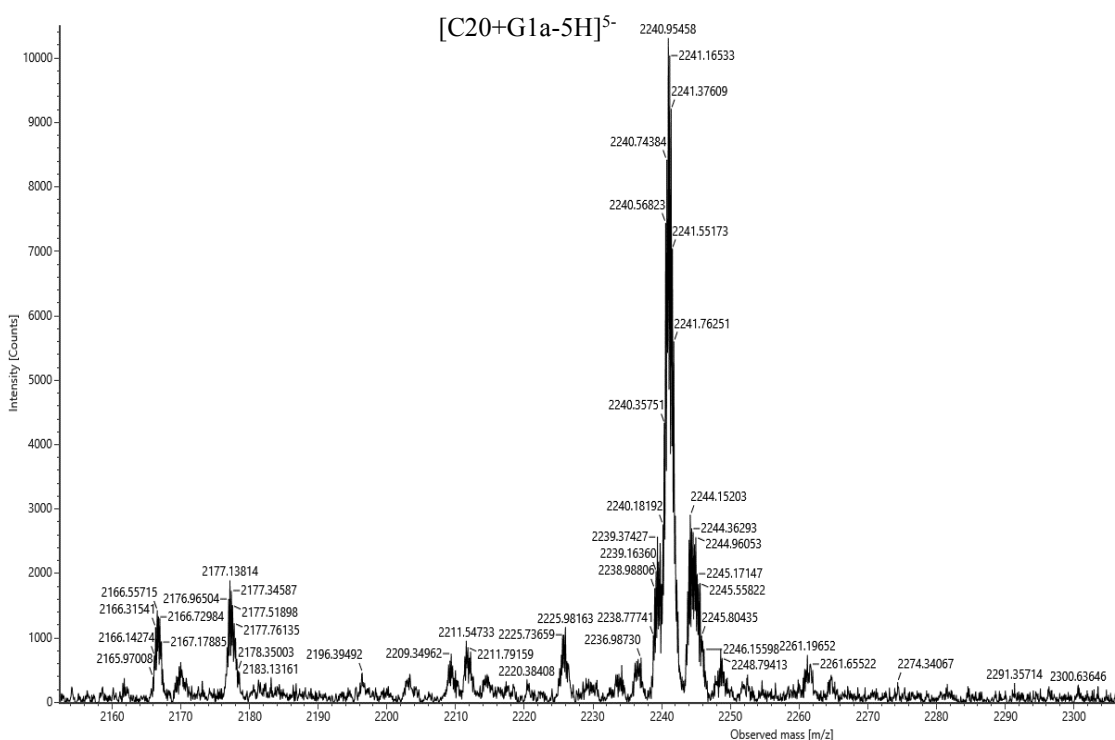
Appendix 5: Mass spectrum of **T19** with G1 aldehyde set in the absence of quinine.



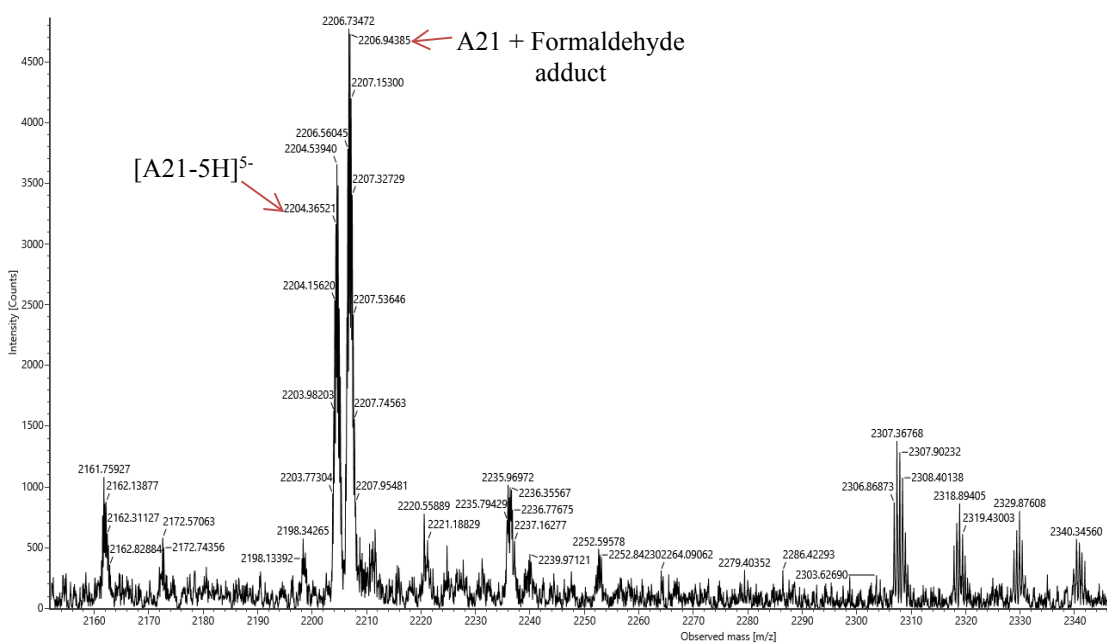
Appendix 6: Mass spectrum of **C20** with G1 aldehyde set in the presence of quinine.



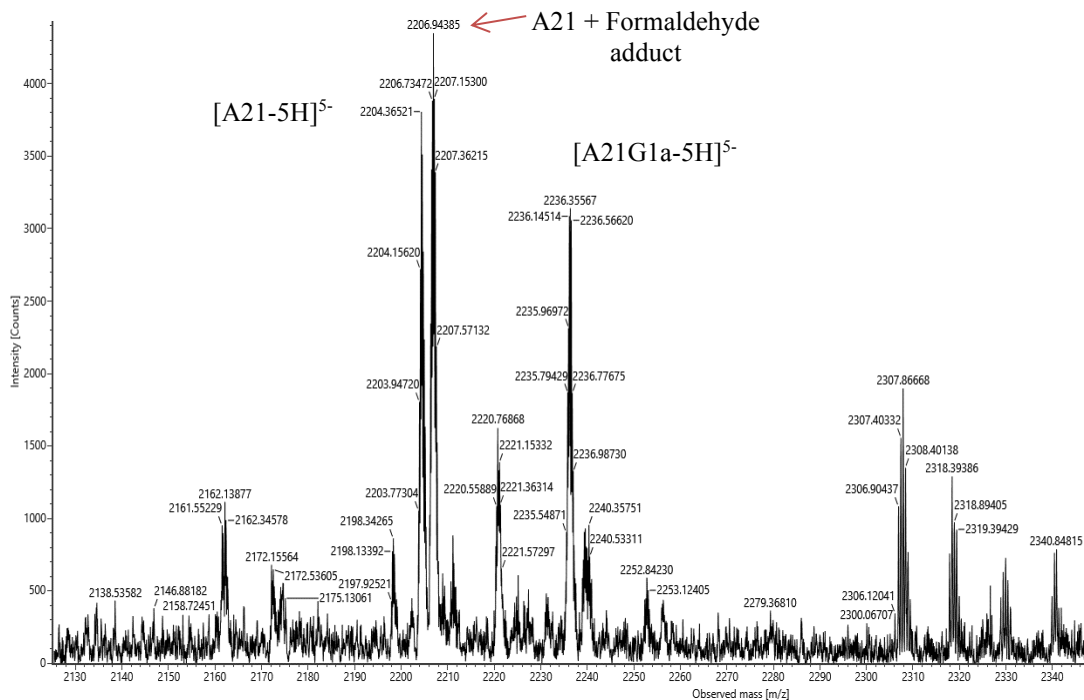
Appendix 7: Mass spectrum of **C20** with G1 aldehyde set in the absence of quinine.



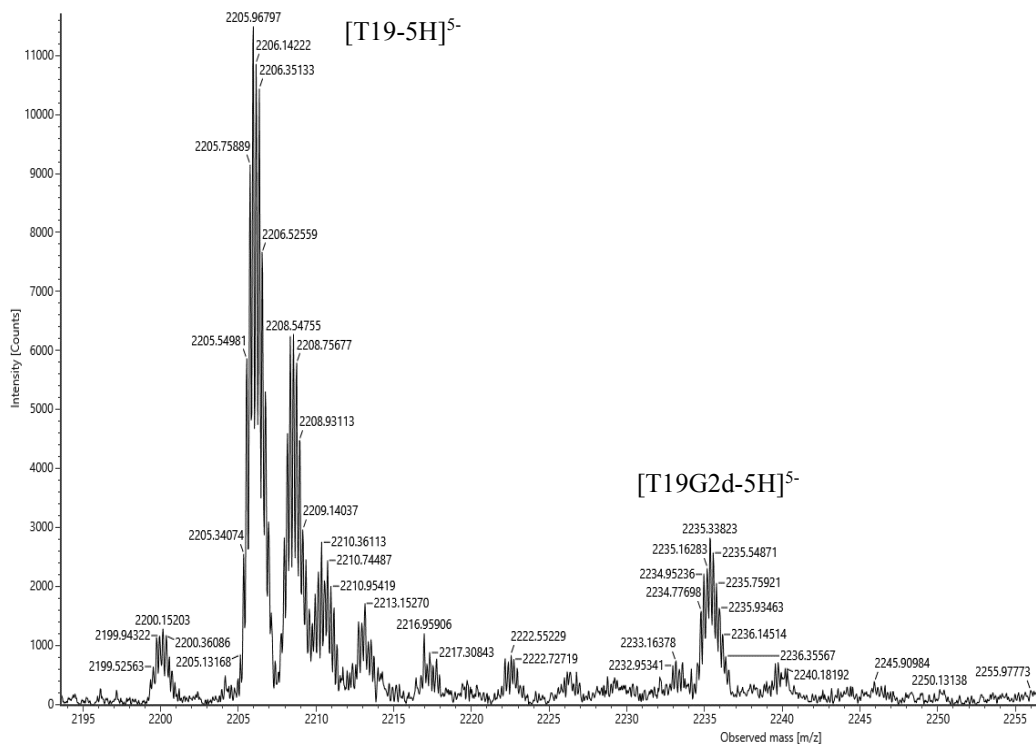
Appendix 8: Mass spectrum of **A21** with G1 aldehyde set in the presence of quinine.



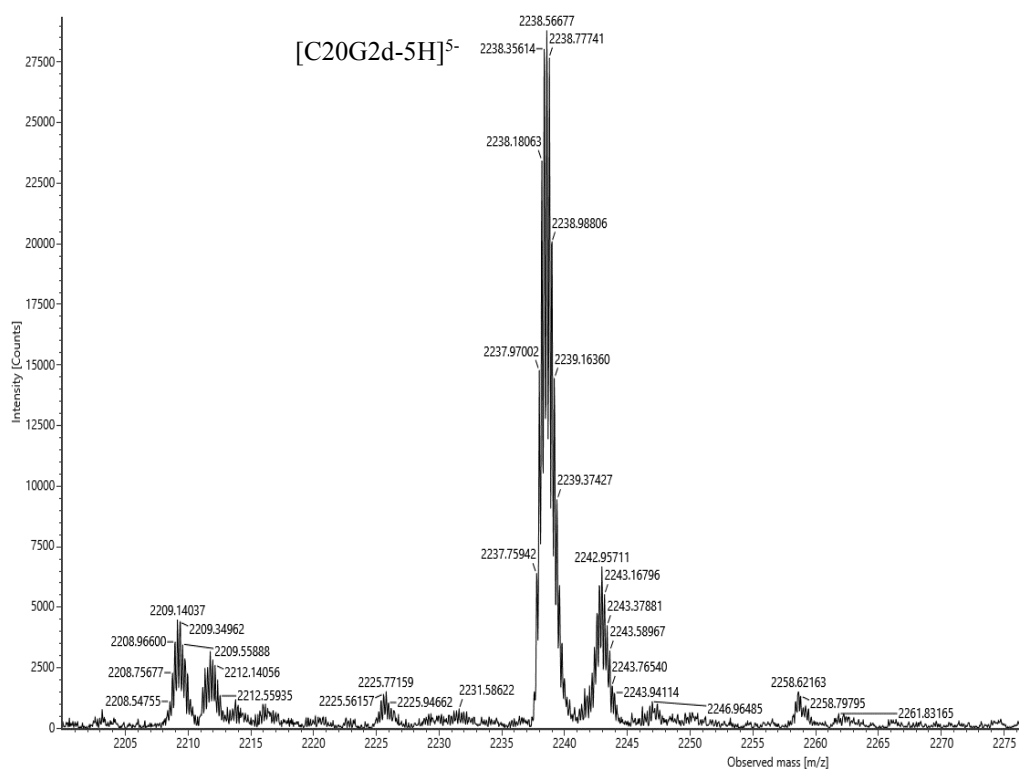
Appendix 9: Mass spectrum of **A21** with G1 aldehyde set in the absence of quinone.



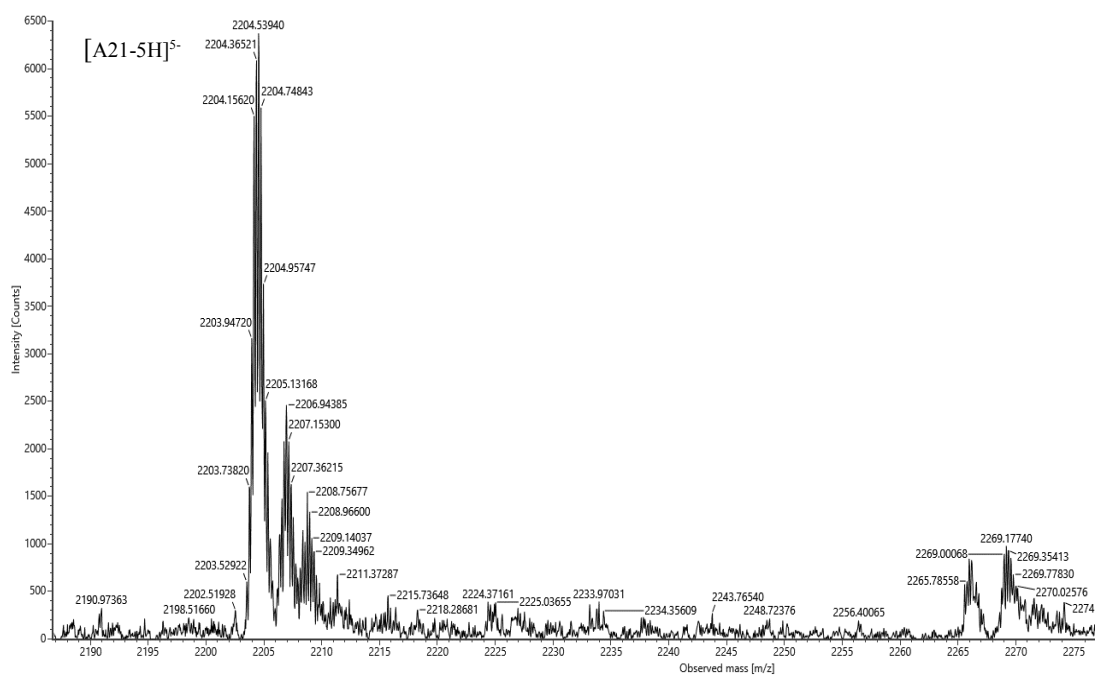
Appendix 10: Mass spectrum of **T19** with G2 aldehyde set in the presence of quinone.



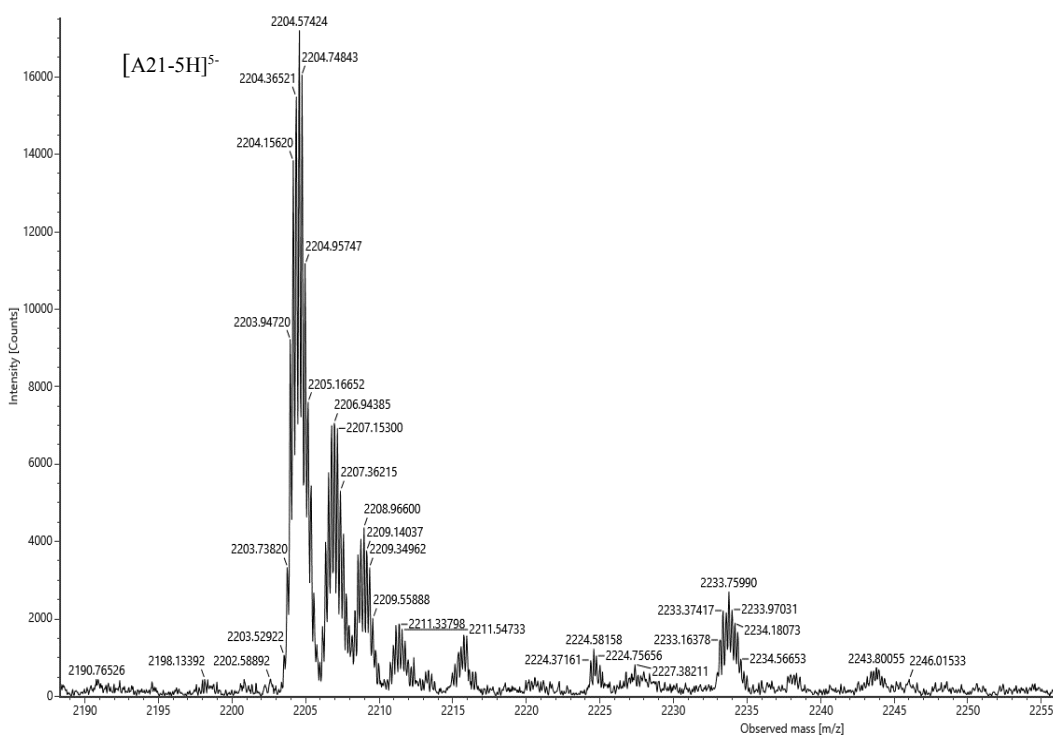
Appendix 13: Mass spectrum of C20 with G2 aldehyde set in the absence of quinine.



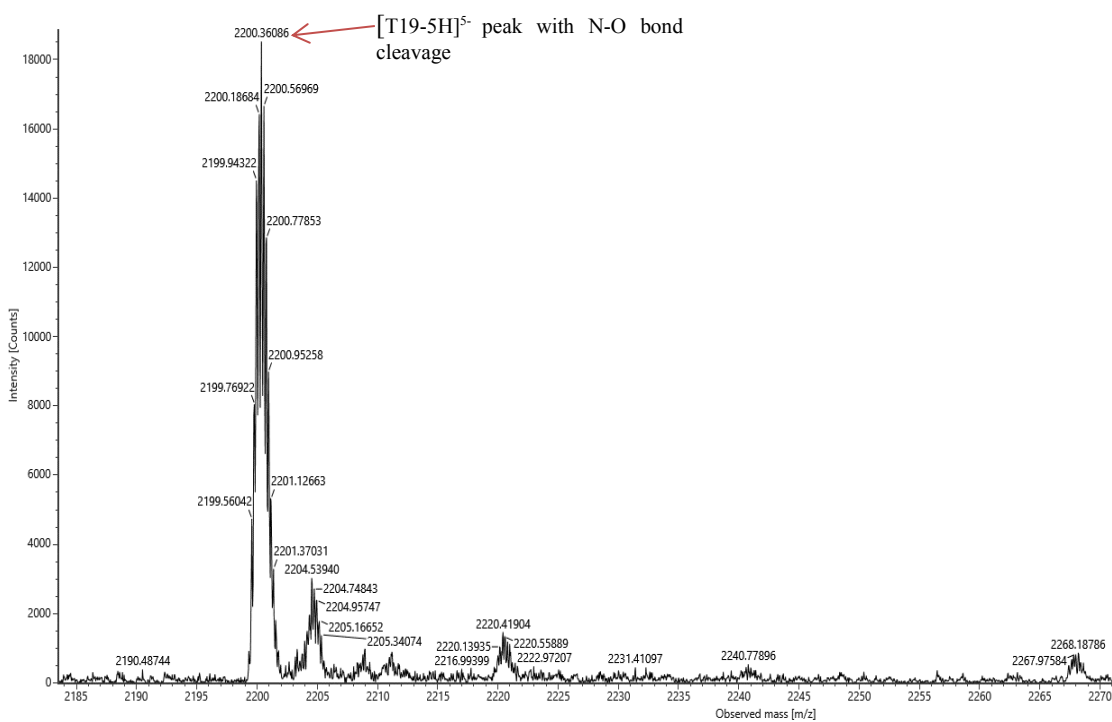
Appendix 14: Mass spectrum of A21 with G2 aldehyde set in the presence of quinine.



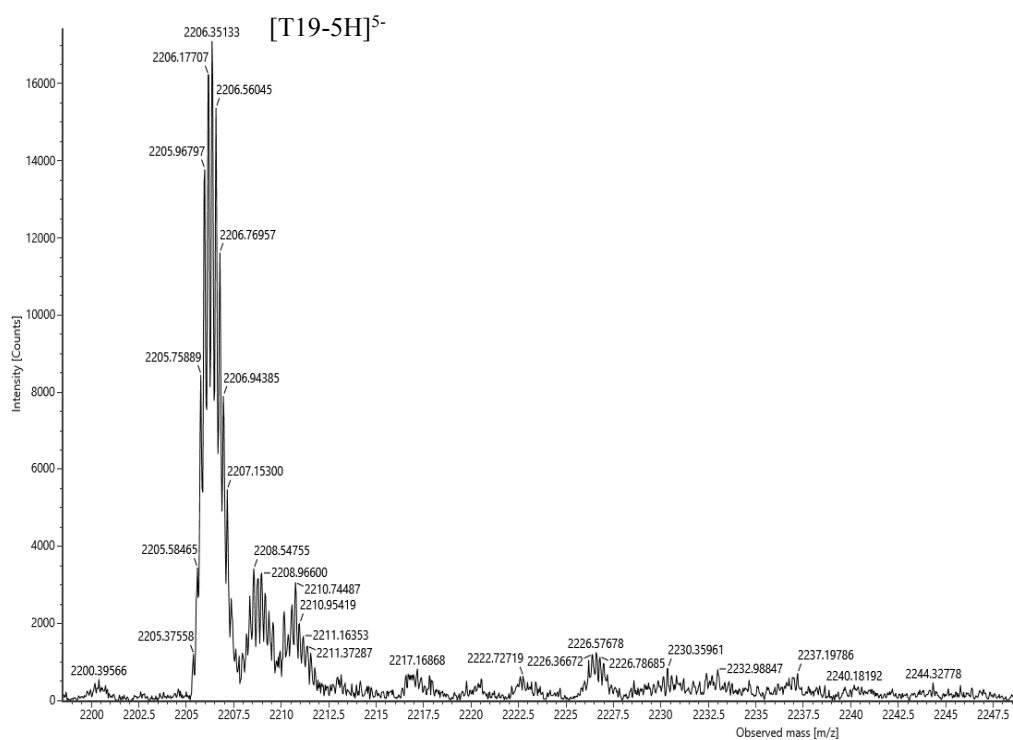
Appendix 15: Mass spectrum of **A21** with G2 aldehyde set in the absence of quinine.



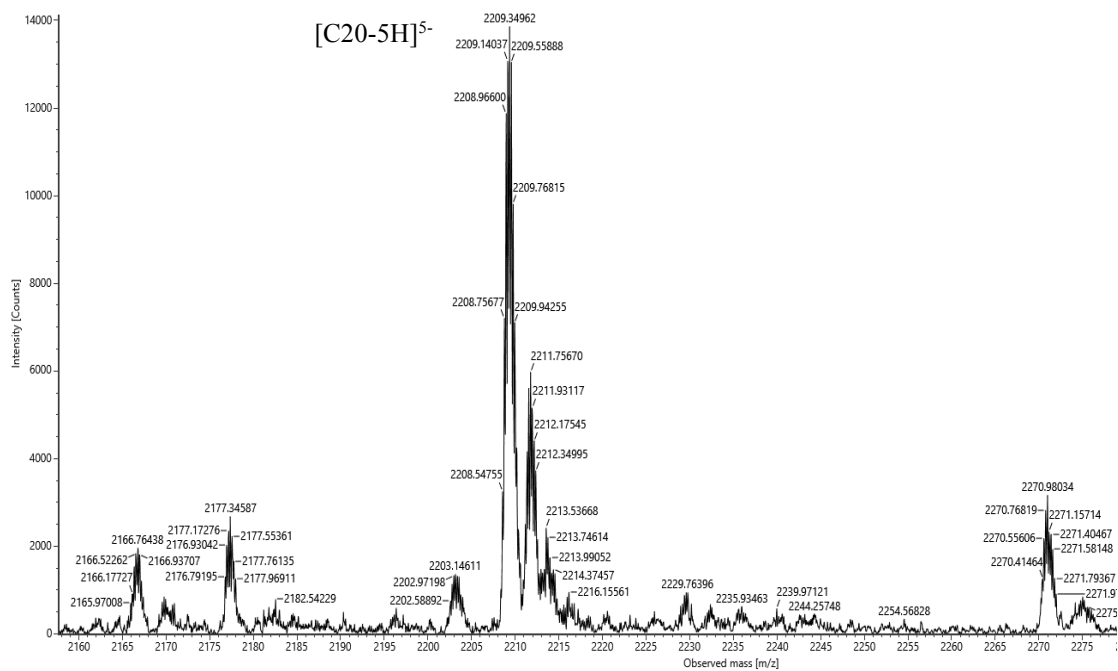
Appendix 16: Mass spectrum of **T19** with A1 aldehyde set in the presence of quinine.



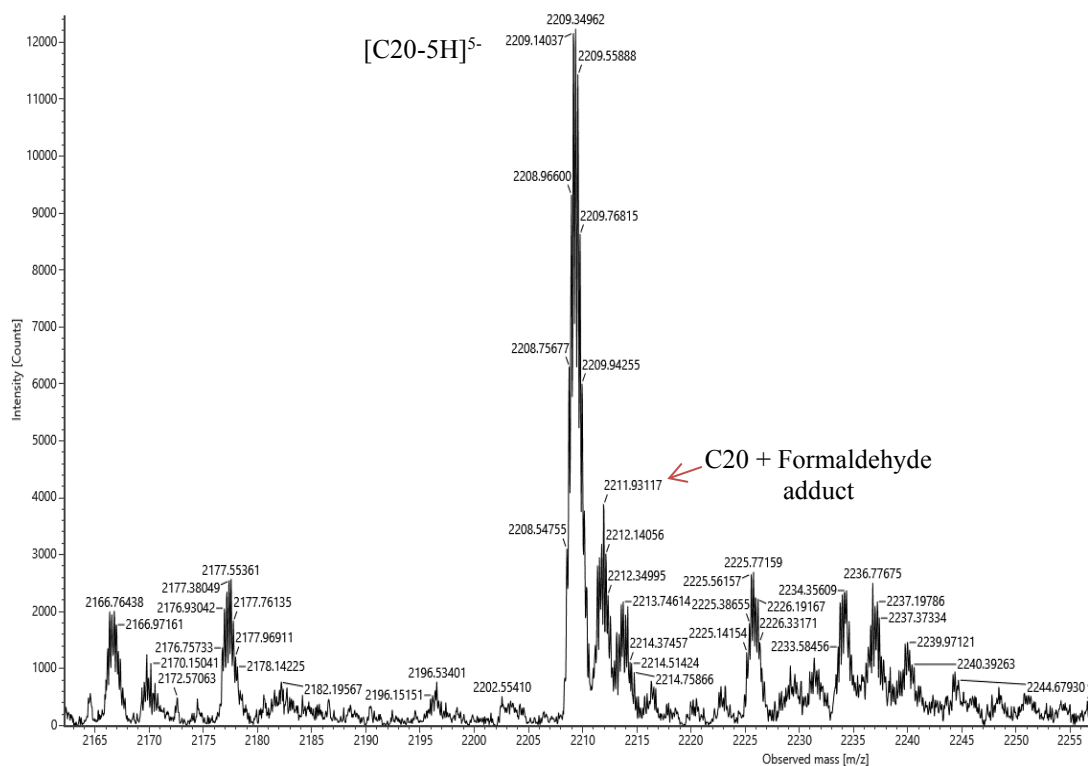
Appendix 17: Mass spectrum of **T19** with A1 aldehyde set in the absence of quinine.



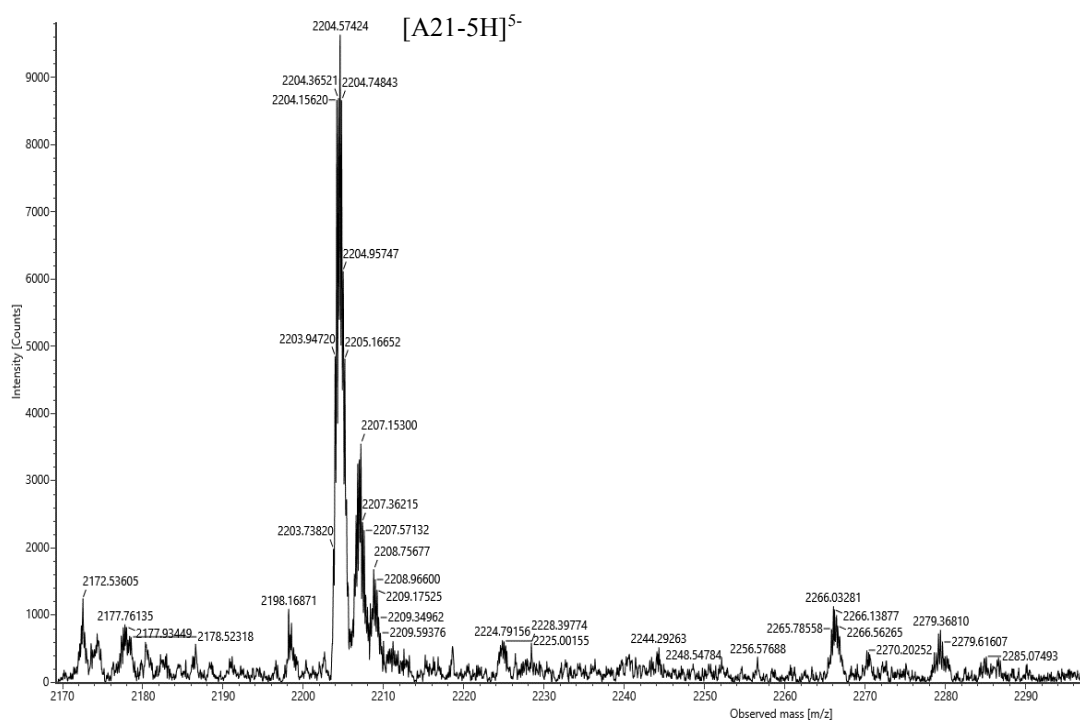
Appendix 18: Mass spectrum of **C20** with A1 aldehyde set in the presence of quinine.



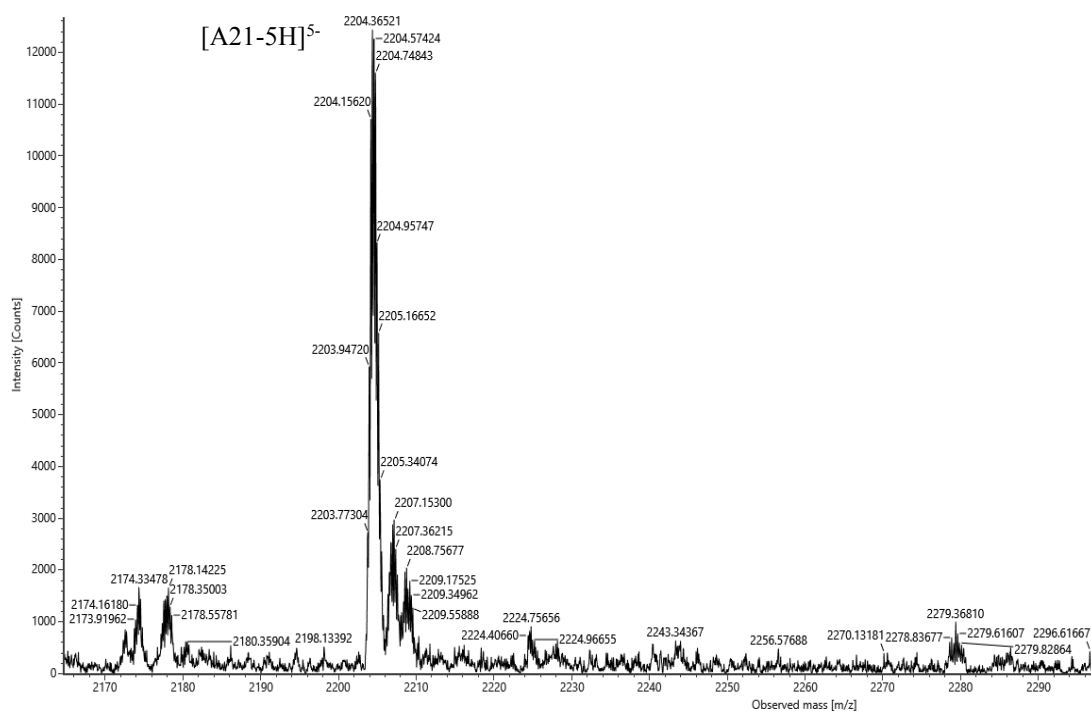
Appendix 19: Mass spectrum of C20 with A1 aldehyde set in the absence of quinine.



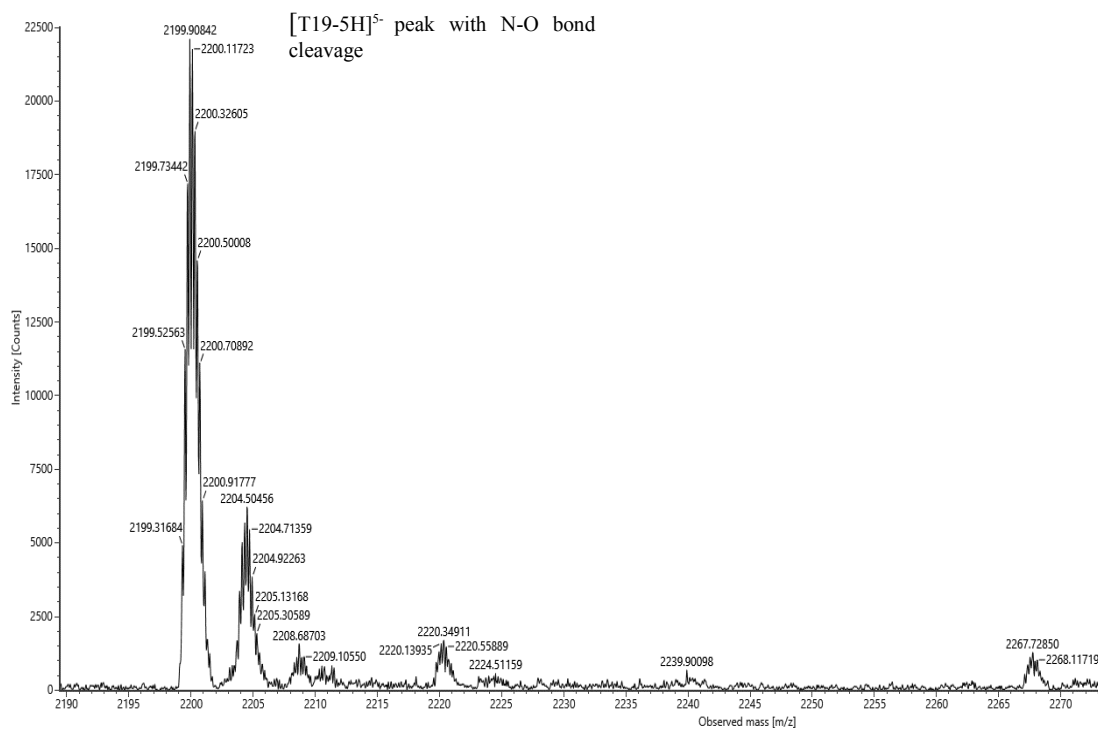
Appendix 20: Mass spectrum of A21 with A1 aldehyde set in the presence of quinine.



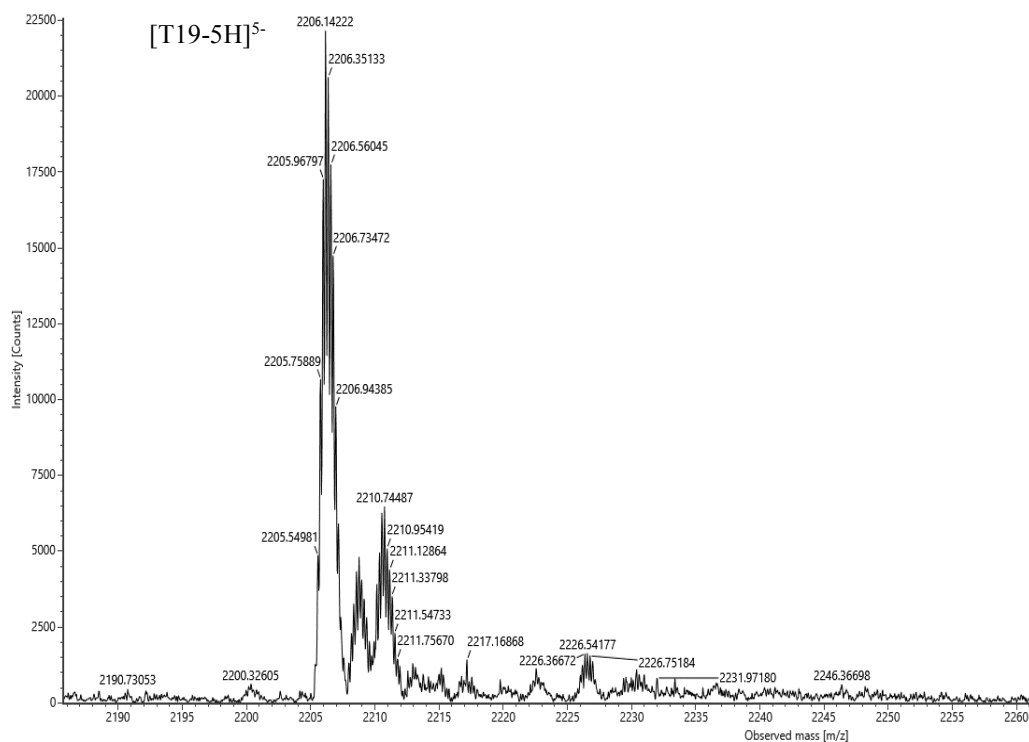
Appendix 21: Mass spectrum of **A21** with A1 aldehyde set in the absence of quinine.



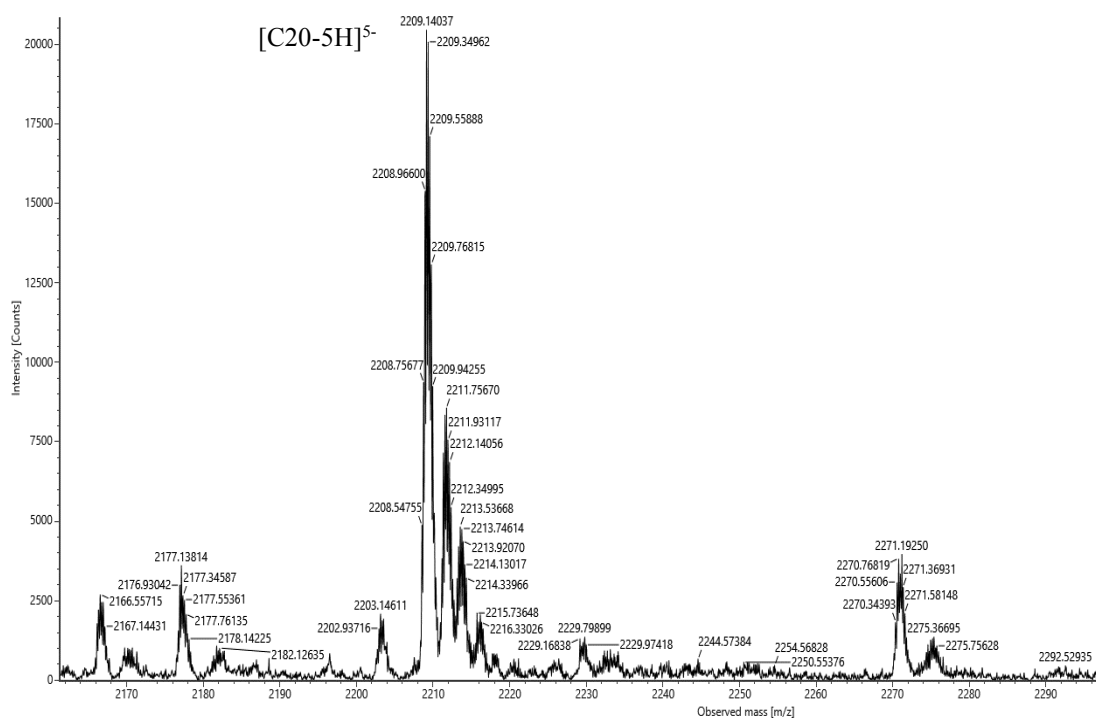
Appendix 22: Mass spectrum of **T19** with A2 aldehyde set in the presence of quinine.



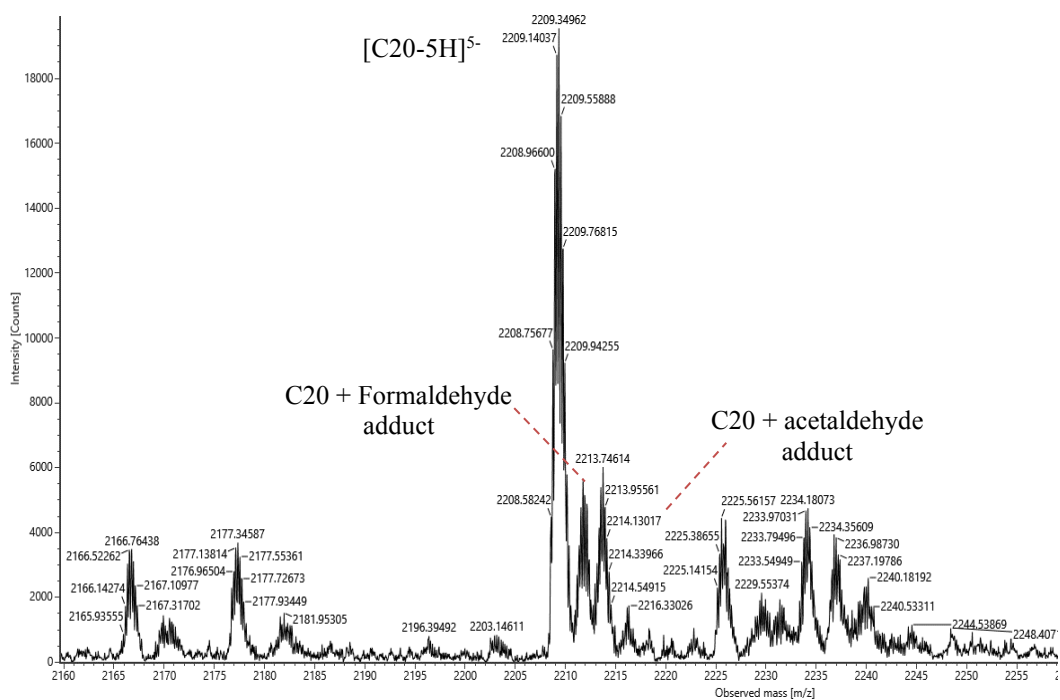
Appendix 23: Mass spectrum of **T19** with A2 aldehyde set in the absence of quinine.



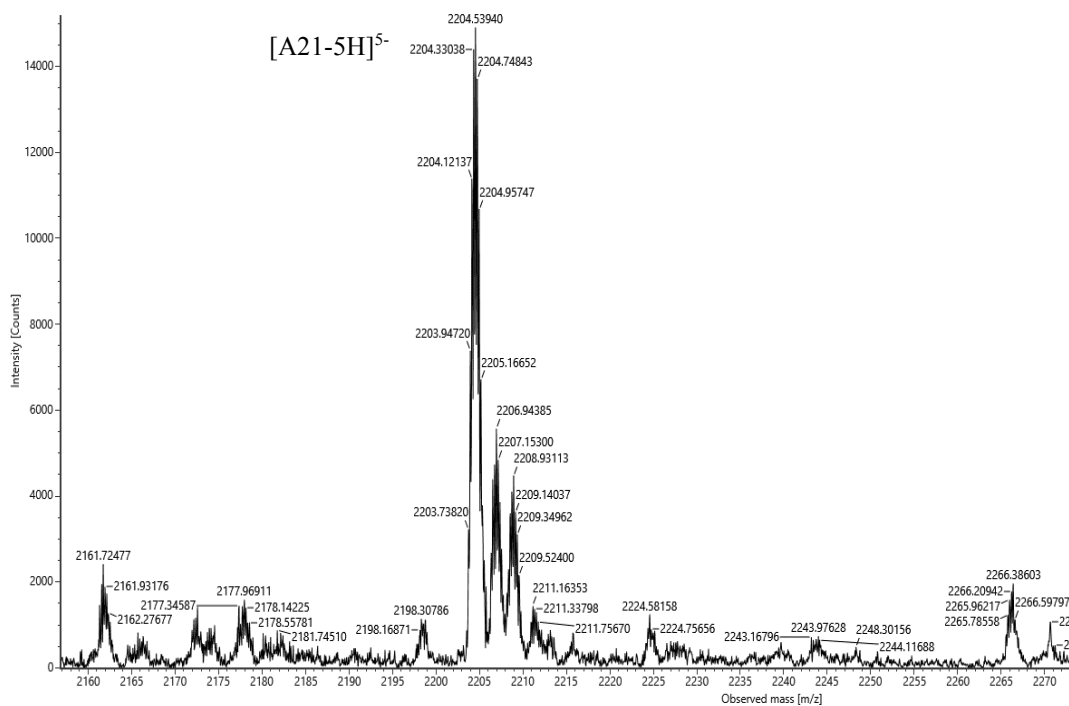
Appendix 24: Mass spectrum of **C20** with A2 aldehyde set in the presence of quinine.



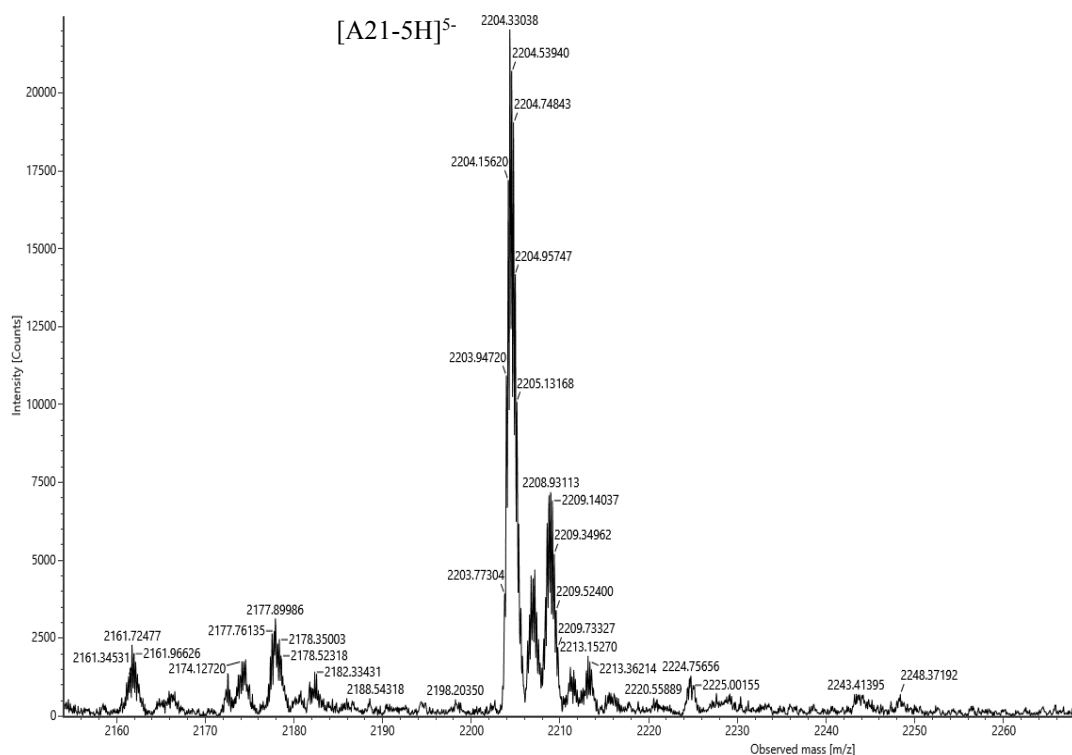
Appendix 25: Mass spectrum of C20 with A2 aldehyde set in the absence of quinine.



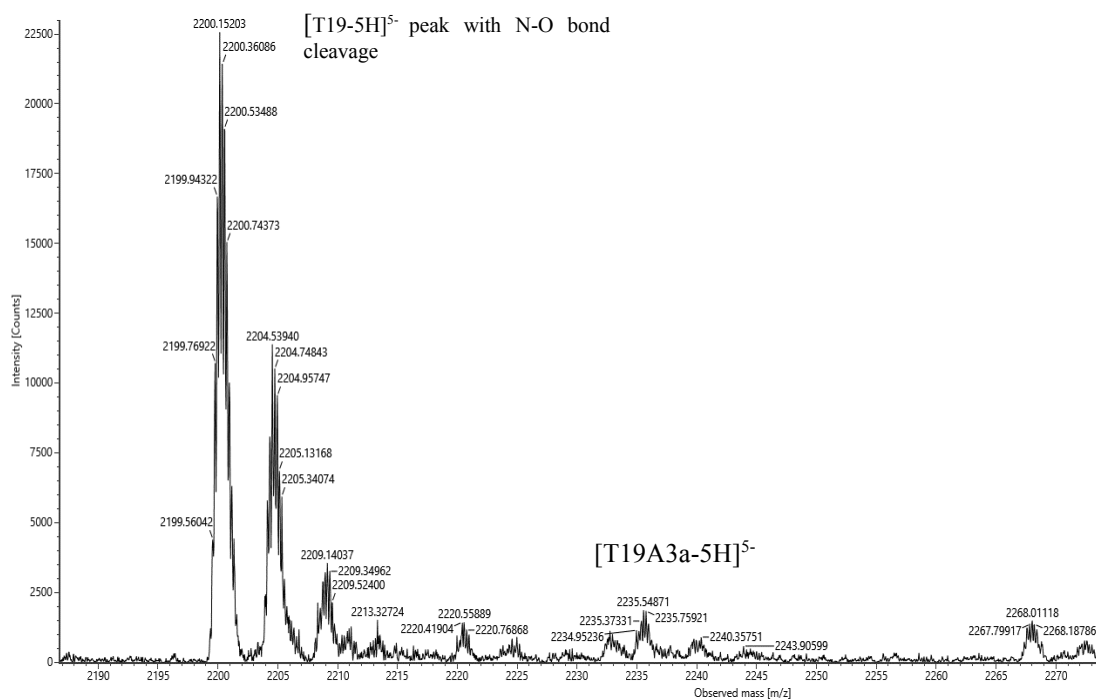
Appendix 26: Mass spectrum of A21 with A2 aldehyde set in the presence of quinine.



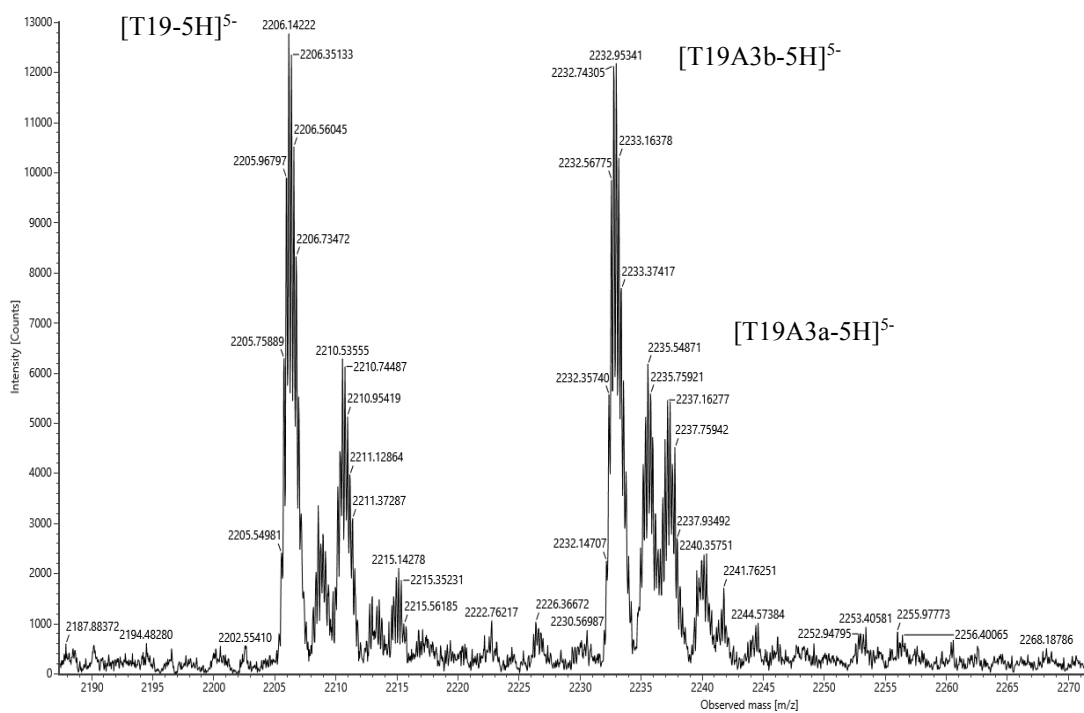
Appendix 27: Mass spectrum of **A21** with A2 aldehyde set in the absence of quinine.



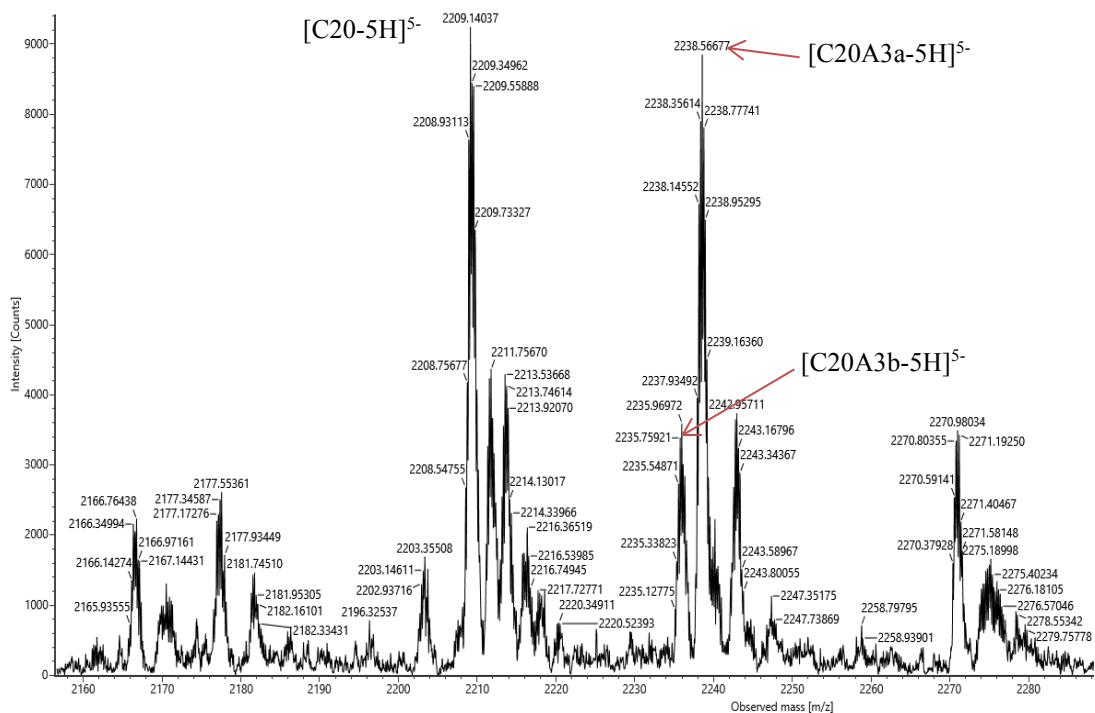
Appendix 28: Mass spectrum of **T19** with A3 aldehyde set in the presence of quinine.



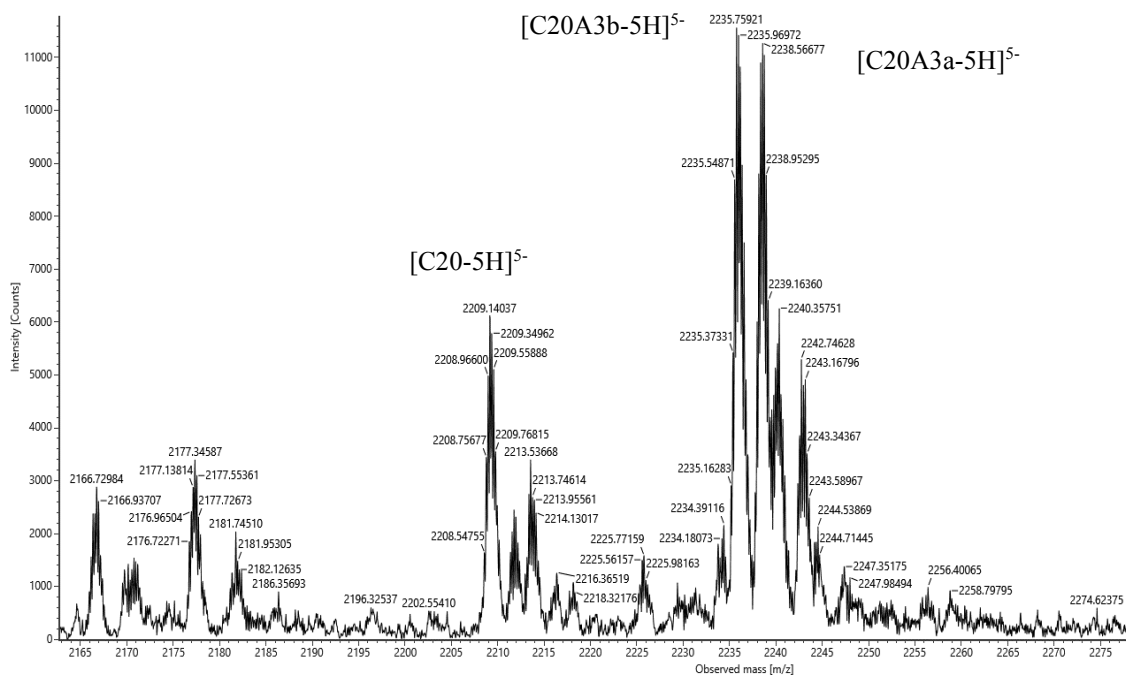
Appendix 29: Mass spectrum of **T19** with A3 aldehyde set in the absence of quinine.



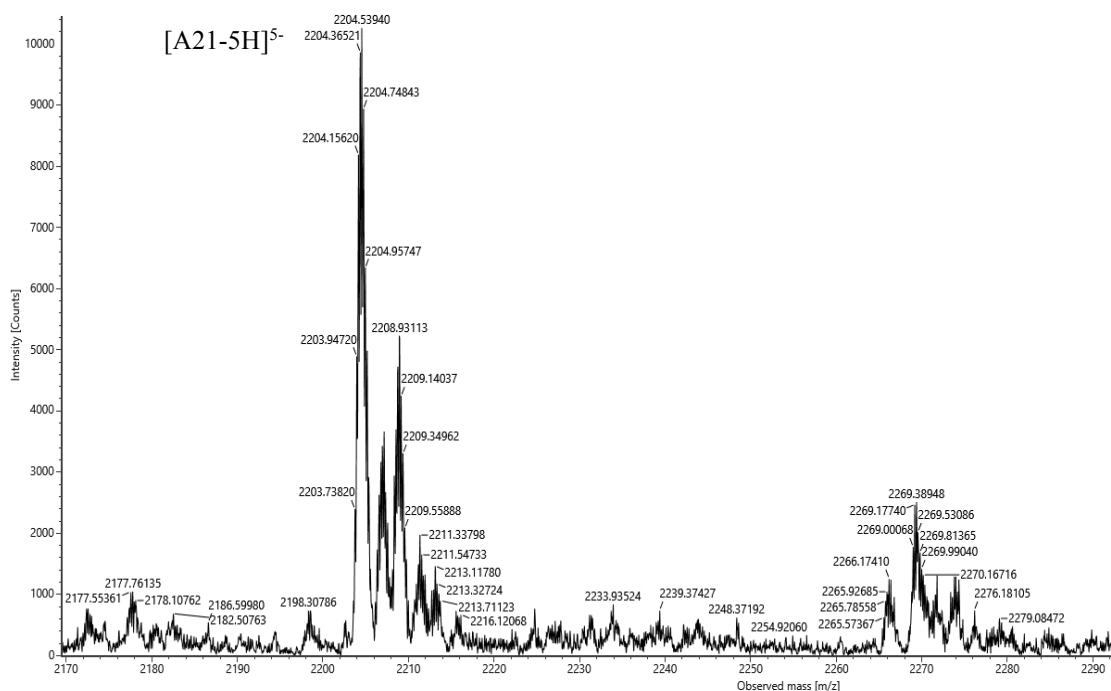
Appendix 30: Mass spectrum of **C20** with A3 aldehyde set in the presence of quinine.



Appendix 31: Mass spectrum of **C20** with A3 aldehyde set in the absence of quinine.



Appendix 32: Mass spectrum of **A21** with A3 aldehyde set in the presence of quinine.



Appendix 33: Mass spectrum of **A21** with A3 aldehyde set in the absence of quinine.

